MSC Thesis

Dissipating phantom traffic jams with haptic shared control for longitudinal vehicle motion

4368924
Klaas Koerten

Delft University of Technology

TU Delft

Dissipating phantom traffic jams with haptic shared control for lontigutinal vehicle motion

MSc Thesis

Klaas Koerten

To obtain the degree of

Master of Science
In Mechanical Engineering

At the
Delft Haptics Lab
Department of Cognitive Robotics
Delft University of Technology

Supervisors:
Prof. dr. Ir. D.A. Abbink
Dr. A. Zgonnikov
July 1, 2021

Assessment Committee

Committee Chair
Prof. Dr. Ir. D. A. Abbink
Department of Robotics
Faculty of 3mE, TU Delft

Supervisor
Dr. A. Zgonnikov
Department of Robotics
Faculty of 3mE, TU Delft

External Member
Dr. Ir. S. C. Calvert
Delft Data Analytics and Traffic Simulation lab
Faculty of Civil Engineering and Geoscience, TU Delft

External Member
Ir. C. Koppel
Cruden Driving Simulators B.V.

Student
K. O. Koerten
Department of Robotics
Faculty of 3mE, TU Delft

This research project was made possible by Cruden Driving Simulators B.V. Their corporation is hereby gratefully acknowledged.

Preface

Traffic jams on highways cause increased travel time as well as increased fuel consumption and emissions. When not triggered by a distinctive cause such as an on-ramp or an accident, they are referred to as phantom traffic jams. This graduation thesis tries to answer the question if phantom traffic jams can be dissolved or prevented using haptic shared control for longitudinal vehicle motion. I carried out this research project at the Delft University of Technology in collaboration with Cruden Driving Simulators B.V. in Amsterdam. The Delft University of Technology was there for the academic part of this research project, while Cruden provided me with both an office space to work as well as state of the art simulator hardware, software and expert knowledge that made this project to a success. This report starts off with a research paper that describes the results and relevance of the final experiments. I included the appendices that follow the paper to provide background on the graduation project as a whole.

I would like to thank my supervisors at the TU Delft, Arkady and David. Arkady was always there to answer my questions very quickly, and to review my writing thoroughly and David, although we seldom met, would always inspire me to dig deeper into the subject. I would also like to thank Cruden for making it possible for me to do my graduation there, especially in these times where many people were forced to work from home. I would like to specifically thank Christiaan for always being available to answer any technical questions I had and Omar and Tim for helping me set up the simulator.

K. O. Koerten
July 1, 2021

Contents

Research Paper **3**

Appendix A: Traffic Controller **13**

Appendix B: Simulator Setup **16**

Appendix C: Data Analysis **19**

Appendix D: Raw Data **27**

Appendix E: Forms **51**

Dissipating Phantom Traffic Jams with Haptic Shared Control for Longitudinal Vehicle Motion

K. O. Koerten, A. Zgonnikov, D. A. Abbink
Cognitive Robotics Dept., Faculty of 3mE, Delft University of Technology

***Abstract* - Traffic jams occurring on highways cause increased travel time as well as increased fuel consumption and crashes. Traffic jams without a clear cause, such as an on-ramp or an accident, are called phantom traffic jams and are said to make up 50% of all traffic jams. They are the result of an unstable traffic flow caused by human driving behaviour. Recent studies have shown how automating the longitudinal vehicle motion of only 5% of all cars in the flow can dissipate phantom traffic jams. However, automation introduces new problems, mainly regarding safety when human drivers need to take over the control. This research tries to answer whether phantom traffic jams can be dissolved or prevented using haptic shared control. This means of control keeps the human in the loop and would therefore eliminate the takeover problems while still benefiting from the advantages of automation. 24 participants took part in a driving experiment in a fixed base simulator. In these experiments, we tested haptic shared control against manual control and full automation for longitudinal motion. Results show that traffic jam dissipation performance for haptic shared control lies between manual control and automation. The number of unsafe situations is reduced compared to the automated condition. We conclude that haptic shared control is able to reduce the increased fuel consumption and crashes caused by phantom traffic jams.**

Keywords: Phantom traffic jams, Haptic shared control, Active pedals, Longitudinal vehilcle motion, Simulator study, Silent automation failure

I. INTRODUCTION

A phantom traffic jam is a phenomenon on a busy road where vehicles drive at much slower speeds than desired or allowed. Traffic jams have far-reaching consequences, such as longer travel times, more crashes and increased fuel consumption and emissions due to the stop-and-go behaviour of vehicles in traffic jams (Mahmud et al., 2012, Wu et al., 2019). Where accidents, sharp curves, on-ramps or sudden lane changes of vehicles cause regular traffic jams, phantom traffic jams occur without a distinct cause. According to Goldmann and Sieg (2020), up to fifty per cent of all traffic jams do not have a distinct cause and are therefore phantom traffic jams. Consequently, possible ways to eliminate phantom traffic jams have been investigated.

Vehicle density plays a crucial role in the formation of phantom traffic jams. Each road has a certain critical density for each velocity. If car density increases beyond this density, the flow becomes unstable, and the average speed of the vehicles drops below the speed limit (Treiber and Kesting (2013)). However, high density is necessary for the formation of phantom traffic jams, but it is not its cause. What triggers phantom traffic jams are velocity oscillations caused by the poor driving behaviour of humans. If these oscillations occur in a traffic flow that is dense enough, this same human driving behaviour can amplify the initial disturbance until a traffic jam forms Lee and Kim (2019). Sugiyama et al. (2008) and Tadaki et al. (2013) have shown this phenomenon occurring on a single lane ring road with no external causes. Initially, drivers manage to keep a constant speed, but after some time, oscillations start to happen and the flow eventually becomes unstable, and stop-and-go waves start to form. These studies show how human driving behaviour is the main cause of the occurrence and preservation of phantom traffic jams. According to Gunter et al. (2020), commercially available adaptive cruise control systems amplify disturbances in a traffic flow just as much as human drivers do. This result shows that the available means to automate longitudinal motion do not solve phantom traffic jams. However, studies aiming to solve phantom traffic jams do exist. We divide the developed solutions into two categories. **Centralised solutions** use sensors in the infrastructure to identify phantom traffic jams and solve them using dynamic traffic signs. Solutions include opening up additional traffic lanes or changing the speed limit. These solutions have been shown to stabilise dense traffic (Hoogendoorn et al. (2013)). However, adaptations to existing infrastructure are required, and dynamic speed limits might slow down traffic when this is unnecessary. **Decentralised solutions** use automated vehicles as agents to stabilise traffic locally to prevent phantom traffic jams before they have formed. One type of decentralised solution lets multiple automated vehicles drive behind one another in a stable *platoon* (Kim et al. (2015)). Another type stabilises a traffic flow with a small number of automated vehicles (typically no more than 10%) equipped with cruise control specifically developed for this (Kreidieh et al. (2018), Stern et al. (2018), Čičić and Johansson (2018)). This last category seems especially promising because it only requires small adaptations to vehicles and works for realistic penetration rates of cars equipped with adaptive cruise control.

However, automating vehicles comes at a cost. When the longitudinal motion of a car is automated, the drivers function as supervisors of the automated system instead of operators, i.e. the human is taken out of the loop (Parasuraman (1987))). Bainbridge (1983) explains that when humans become supervisors instead of operators, their skills as operators of the task decline over time. However, they remain responsible for taking over the task when things get too complicated for the automation. Typical problems associated with automation are the vigilance decrement, where the drivers' attention declines over time and overreliance. Here, the driver has put too much trust in the automation and does not take over when necessary (Parasuraman (1987)). Other disadvantages are increased reaction times and decreased performance when the human needs to take over. Human drivers sometimes do need to take over, because adaptive cruise control systems may experience difficulty in tracking a leading vehicle (Son et al. (2006)), or in identifying an approaching stationary queue (Nilsson (1996)). In these cases, the human drivers need to intervene. Rudin-Brown and Parker (2004) show that reaction times of drivers increase when they rely on adaptive cruise control. These combined effects could result in unsafe driving situations, especially in the dense traffic situations in which phantom traffic jams occur.

Humans need to take over control from time to time as long as automation is not yet perfect. Preventing the downsides of automation, as mentioned above, requires humans to stay engaged in the driving task. Continuously sharing the control between the human operator and the automation ensures driver engagement while still benefiting from the advantages of automation. In a simulator study, Jiang et al. (2021) show how a sharing algorithm dampens traffic waves on a circular ring road. This shared controller calculates the average control input of the human and an automated feedback controller, which is the input for the velocity controller. However, this controller lacks a way in which the human and the automation can communicate, which would allow the human operator to obtain information about the control action of the automation. Shared control that does allow for this communication, is haptic shared control, where both the human operator and the automation exert forces on a control surface. The position of this control surface then determines the control action (Abbink and Mulder (2010)). Research by Flemisch et al. (2008) has already pointed out that haptic shared control for lateral vehicle motion can significantly improve safety compared to full automation when a silent automation failure happens. Previous research has reported improved performance with haptic feedback on the accelerator pedal for car-following (Mulder et al. (2008)), for making drivers more compliant to speed limits (Adell et al. (2008)) and for promoting a more eco-friendly driving style (Azzi et al. (2011), Jamson et al. (2013)).

This research aims to evaluate the efficacy of haptic shared control for dissipating phantom traffic jams. We will design a haptic shared controller, which we will test in driving simulator tests with 24 participants. As benchmarks, we evaluate the manual and fully automated conditions. The participants will also subjectively grade the haptic and automated system.

II. HAPTIC SHARED CONTROLLER DESIGN

The proposed haptic shared controller requires both software and hardware components. The software is essential to simulate the driving environment and to calculate the haptic forces that the controller applies to the pedals. The hardware design is necessary to provide a physical interface where a human operator can interact with the automation.

1) SOFTWARE DESIGN

To implement haptic shared control, we first calculate the ideal longitudinal motion for the tested scenario. We took the algorithm that we use from Stern et al. (2018). In this study, Stern et al. use the algorithm to calculate an ideal speed based on the bumper-to-bumper gap and velocity difference between the ego vehicle and the leading vehicle. The speed is then fed into the cruise controller of the controlled car. We calculate the ideal speed in the following way:

$$v^{cmd} = \begin{cases} 0 & \text{if} \quad \Delta x \leq \Delta x_1 \\ v\frac{\Delta x - \Delta x_1}{\Delta x_2 - \Delta x_1} & \text{if} \quad \Delta x_1 < \Delta x \leq \Delta x_2 \\ v + (U - v)\frac{\Delta x - \Delta x_2}{\Delta x_3 - \Delta x_2} & \text{if} \quad \Delta x_2 < \Delta x \leq \Delta x_3 \\ U & \text{if} \quad \Delta x_3 < \Delta x \end{cases} \tag{1}$$

where

$$\Delta x_k = \Delta x_k^0 + \frac{1}{2d_k}(\Delta v\_)^2, \quad \text{for} \quad k = 1, 2, 3 \tag{2}$$

In these equations, v^{cmd} is the demanded speed, U is the maximum speed on the road, Δx is the bumper-to-bumper gap between the ego and leading vehicle, v is the current speed, and $\Delta v\_$ is the difference in longitudinal velocity between the ego and leading vehicle. Δx_k^0 and d_k are constant parameters, directly taken from Stern et al. (2018): $\Delta x_1^0 = 4.5m$, $\Delta x_2^0 = 5.25m$, $\Delta x_2^0 = 6.0m$, $d_1 = 1.5\frac{m}{s^2}$, $d_2 = 1\frac{m}{s^2}$ and $d_3 = 0.5\frac{m}{s^2}$. As equation 1 shows, the calculated velocity is either 0, a value between 0 and the current velocity, a value between the current velocity and the maximum velocity or the maximum velocity. What determines v^{cmd} is based on the gap, Δx and Δx_k, of which the value depends on a certain base gap, Δx_k^0 with an added term based on the velocity difference between the two vehicles, $\Delta v\_$. Stern et al. (2018) provide a more detailed description of this algorithm.

The difference between v^{cmd} and v is the input for the pedal controller. This controller does the following:

$$\begin{aligned} if \quad & v^{cmd} - v > 0 \Rightarrow \text{accelerate} \\ if \quad & 0 \geq v^{cmd} - v \geq -0.25 \Rightarrow \text{do nothing} \\ if \quad & v^{cmd} - v < -0.25 \Rightarrow \text{brake} \end{aligned} \tag{3}$$

Equation 3 shows that the control actions are either to **1)** do nothing, making the car brake on the engine, where both pedals get released, **2)** press the accelerator pedal and release the brake pedal to accelerate or **3)** press the brake pedal and release the accelerator pedal to decelerate. When acceleration or deceleration needs to happen, the pedal position of the accelerator or the brake pedal is determined by feeding the difference in speed into the accelerator or decelerator controller respectively. Both controllers are PID controllers that produce the ideal pedal positions, S^{ideal}_{acc} and S^{ideal}_{brake}. The gains of the accelerator controller are $Kp = 1$, $Ki = 0.01$ and $Kd = 0.05$ and the gains of the decelerator controller are $Kp = 0.7$, $Ki = -0.04$ and $Kd = 0.1$. Appendix A displays a more detailed description of these controllers.

The accelerator and brake pedal that we use are control interfaces using control loader technology. Software controls the virtual mass, damping, stiffness and the forces that the pedals exert on the driver's foot. The default behaviour of both pedals is spring-damper behaviour. We calculate the force F^{pedal} that gets applied to the driver's foot by the pedal by taking the product of the pedal position S^p and pedal stiffness K and adding this to the product of the pedal speed v^p and damping b. We use Spring-damper pedal behaviour in the manual control situation for both the accelerator and the brake pedal.

For the haptic shared controller we use the difference between the current pedal position $S^{current}$ and the ideal position S^{ideal} to either increase or decrease the stiffness of the accelerator pedal. Figure 1 shows a block diagram of this. We multiply the difference between the current and ideal pedal positions with a haptic stiffness K^h, and add the resulting value to the initial stiffness K. The choice to use stiffness feedback as opposed to, for example, force feedback was made based on the paper by Mulder et al. (2010). In pilot studies, participants reported that haptic feedback on the brake pedal did not make them feel safe in the car. This was because a braking action is done to quickly slow down the car. When the driver would want to press the brake sooner or later than the automation, the brake would be less stiff or stiffer than expected. This would result in unwanted behaviour of the brake pedal and therefore in an unwanted braking action, making the driver feel unsafe.

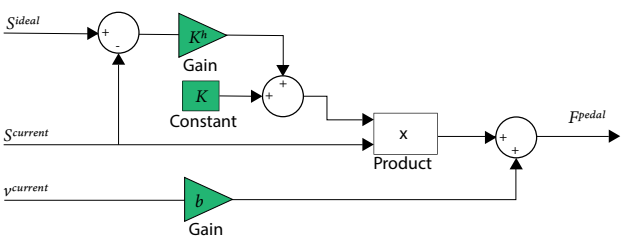

Figure 1: Block diagram of the accelerator pedal for the haptic shared control case

That is why we made the choice to only provide haptic feedback on the accelerator pedal. Also, we set the increase in stiffness when the pedal needs to be released at $300N/radian^2$ while the decrease in stiffness when the pedal needs to be pressed is to $30N/radian^2$. We base this design choice also on pilot studies where the participants did not notice feedback when the gains were the same for increasing and decreasing the pedal stiffness.

For the automated controller, a force is applied to the pedals proportional to the difference between the pedal position and the ideal pedal position. This forces the pedals in the ideal position. The accelerator as well as the brake pedal are automated for this. Block diagrams for the pedal forces for the manual and automated condition, as well as a more elaborate description of the software setup can be found in appendix A.

Figure 2: The active accelerator and brake pedals, in the front and back respectively. The pedals are both connected to a control loader via a metal rod. Halfway the metal rod, a force cell is placed.

2) HARDWARE DESIGN

Figure 2 shows a picture of the active pedals mentioned before. We built them out of an Audi pedal interface. The pedals are connected to a servo motor via a metal rod, with an axial force sensor placed in the middle of it. This setup is called a control loading system. A feedback loop, closed with the axial force sensor, controls the force that the servo motor applies to the linkage. The rest of the simulator we use in this study was custom built at the Cruden workshop to include the active pedals. This fixed base simulator consists of a car seat, a frame onto which the pedals, a steering

wheel, a single 1920x1080 resolution monitor display, speakers and a set of computers on which the simulation runs. Figure 3 shows a picture of the fixed base simulator. The simulation software we use is IPG carmaker and the simulation is integrated with the Cruden system integrator software, Panthera. This software combines the steering wheel and pedal control inputs, the audiovisual rendering, and the simulated scenario into one coherent realtime simulation. A more elaborate description of the simulator can be found in appendix B.

Figure 3: The fixed base simulator setup.

III. EXPERIMENTAL EVALUATION

1) EXPERIMENT SETUP

We evaluate the haptic shared controller in a ring road scenario with a radius of 42 meters and 21 cars on it (including the ego vehicle). This scenario is based on earlier studies that observe traffic jam formation on ring roads. Both Sugiyama et al. (2008) and Tadaki et al. (2013) observed the formation of phantom traffic jams in similar ring road scenarios and Stern et al. (2018) present a control algorithm to dampen traffic waves for a ring road. We took the circumference and amount of cars in our scenario from Stern et al. (2018) because the Δx_k^0 and d_k parameters from equation 1 are tuned specifically for this scenario. Figure 4 shows a birdseye screenshot of the simulated environment. After four pilot studies, we decided not to let the cars in the simulation start equally spaced around the ring road but to concentrate them behind the ego vehicle at the start of the experiments.Because of this, there is an initial traffic jam that the driver drives into, allowing the traffic jam dissipation of the different means of control to be evaluated. The same human driving algorithm controls the 20 traffic cars in each condition. This standard driver model is the *IIDMACC* model from Treiber and Kesting (2013), with some slight adjustments, of which the reference guide of IPG Carmaker shows the details.

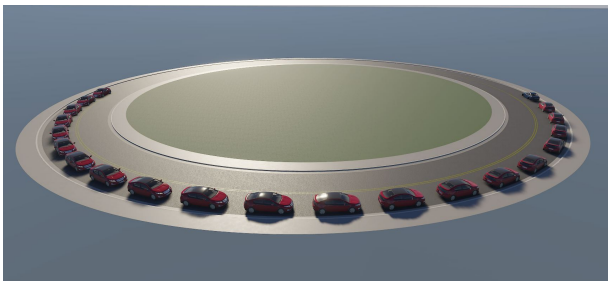

Figure 4: Birdseye view of the simulated ring road environment. The blue car is the ego vehicle and the red cars are the simulated traffic cars.

The experiments consist of 3 driving sessions of 8 minutes during which we ask participants to drive on the simulated ring road. During each session, we test a different controller (manual, haptic or automated). Before the sessions start, participants drive in the manual condition for a couple of minutes to get used to the controls and the simulator. The order in which the conditions are tested varies per participant to eliminate learning effects. During the manual and haptic condition, participants are instructed to control the steering wheel and the pedals themselves. In the automated condition, they only steer and watch the road, as both pedals are automated. Participants only need to interfere with the pedals when a situation is deemed unsafe. After 8 minutes, an automation failure occurs in the haptic and automated condition, corresponding to the real-life situation where the camera system fails to detect the leading vehicle. We simulate this by sending a value of 1000 meters for the bumper-to-bumper gap to the velocity controller, resulting in a v^{cmd} equal to U, causing the haptic accelerator pedal to decrease its stiffness and the automated pedal to get depressed. When this happens, the driver needs to intervene to keep the vehicle safe. After the driver regains control of the car, we terminate the driving session.

To compare the three different means of control, we calculated metrics from the signals recorded during the simulations. The traffic jam dissipation properties of the controllers are analyzed by first looking at how the different means of control influence the stability of the ego vehicle. Metrics for this are the standard deviation of the velocity of the ego vehicle and the amount of braking instances. We chose Braking instead of accelerating because, during a driving task, a driver continuously presses the accelerator pedal. In contrast, the brake pedal is only pressed when a driver wants to slow the vehicle down quickly. Braking has a more drastic effect on the vehicle's speed. Also, braking actions are associated with causing phantom traffic jams (Wismans et al. (2015)). We calculated the braking instances by counting the number of peaks in the signal of brake pedal depression. Next, the influence on the stability of all the vehicles is quantified. The metric for this is the mean standard deviation of the velocity, which we produce by calculating the standard deviations of the velocity signals of all the vehicles and taking the mean of these

values. We use traffic jam lifetime as a metric to evaluate how the different controllers influence the stop-and-go wave dissipation. We calculate the lifetime by taking the moment at which none of the cars stands still anymore. From this moment on, all the cars move and the stop and go wave is dissipated. When this lifetime is 480 seconds, the traffic jam is not solved. To quantify the influence the controllers have on travel time, we use the vehicle throughput as well as the mean speed of all the vehicles as metrics. We calculate Throughput by counting the number of cars that have passed the origin of the ring road during the driving session and dividing this amount by 8 to obtain the average amount of vehicles that drive past the start of the road per minute. Mean speed we calculate by taking the mean of the speed values of all the cars and then taking the average value of these means. We record the bumper-to-bumper gap between the ego vehicle and the leading vehicle to evaluate the safety during the automation failure for the haptic and the automated condition. We use the minimal bumper-to-bumper gap after 480 seconds as a metric and the occurrence of a collision, which happens when the gap value drops below 0. After the experiment, we ask participants to fill out a Van der Laan acceptance form for the haptic and the automated control system. This questionnaire is an instrument to evaluate the acceptance of new technology (Van Der Laan et al. (1997)) and quantifies how the participants subjectively grade the two systems in terms of usefulness and satisfaction. The questionnaire consists of 9 questions where the participants grade the system on a five-point scale from -2 to 2. The complete questionnaire can be found in appendix E.

We perform statistical t-tests to quantify the significance of the controllers on the metrics mentioned above. On the metrics that represent values, we perform a paired t-test. These metrics are the standard deviation of the speed of the ego vehicle, the number of braking instances, mean standard deviation of the velocity of all the cars, traffic jam lifetime, minimal gap and the acceptance scores from the Van der Laan questionnaires. The t-tests produce a t statistic and a p-value, representing the difference in the metric values and therefore quantifying the significance of applying different controllers. For the metrics representing the occurrence of an event, we perform a McNemar test. These metrics are the events in which the traffic jam is solved and the events in which a collision happens after an automation failure. McNemar tests produce a p-value as well as a $Mcnemar \quad \chi^2$) value to quantify the significance. For the t-test as well as the McNemar test, we deem the difference in metric values significant when the p-value is lower than 0.05 (McNemar (1947)). More information about the statistical tests can be found in Appendix D.

HYPOTHESES

We hypothesise that the haptic shared controller increases the stability of the individual vehicle and the traffic flow as a whole and therefore reduces the traffic jam lifetime and the number of times the traffic jam is not dissipated. The haptic shared controller also results in higher average speeds and throughput. We hypothesise that the haptic shared controller improves these properties compared to the manual case but that the automated case improves them even further. When the automation failure happens, we hypothesise that, for the haptic shared control case, the minimal gap increases and that the amount of collisions decreases compared to the automated case.

2) RESULTS

Figures 5, 6, 7 and 8 show signals from the experiments of participant 26, a typical participant. The displayed signals start at 75 seconds, because the experiments start with transient behaviour, where the vehicles drive on the empty road until they enter the traffic jam. At the start of the experiments, this results in signal values for the gap and the velocity that are much higher than those during the rest of the experiment. Plotting these signal values for the entire experiment would make them difficult to compare. Hence the choice is made to cut the signals at 75 seconds. A more elaborate motivation can be found in appendix D. Figure 5 shows the bumper to bumper gap between the ego and the leading vehicle for each condition. The figure shows that in the manual and haptic case, the driver is free to determine this gap, while in the automatic case, shown in figure 5c, the algorithm keeps the gap at a constant value of 6.5 meters. Figure 6 shows velocity trajectories for all three tested conditions. The velocity in the manual case, as shown in figure 6a, oscillates between standstill (0 m/s) and the speed limit (7 m/s). After about 320 seconds, the vehicle does not stop anymore. The stop and go wave is dissipated manually and the car drives at a velocity that oscillates around $4m/s$. The haptic shared control condition in figure 6b shows similar oscillatory behaviour at the start of the experiment, but this already stops after 120 seconds. Finally, the automatic condition shows a velocity signal that oscillates around $4m/s$ during the entire experiment, meaning that the traffic jam that is present at the start of the experiment is dissipated in less than 75 seconds. Figure 7 shows the input signals of the ego vehicle for the three different conditions. Positive values correspond to accelerator pedal depression and negative values to brake pedal depressions. This figure illustrates how, for this participant, the braking instances reduce when comparing haptic shared control and automation with manual control. It also shows how the accelerator pedal positions for both the manual case and the automatic case are more extreme than those of the haptic case. For the manual and automatic case, the pedal values go beyond 50% depression, even after the traffic jam has already been solved. Figure 8 shows how the behaviour of one single controlled vehicle influences the collective behaviour of all the vehicles in the traffic flow. The velocity trajectories of the following and leading vehicle in figure 8a and 8c respectively are similar to those of the ego vehicle while their human driving algorithms is not changed over the different conditions. Signals as shown in figures 5, 6, 7 and 8 from all of the participants

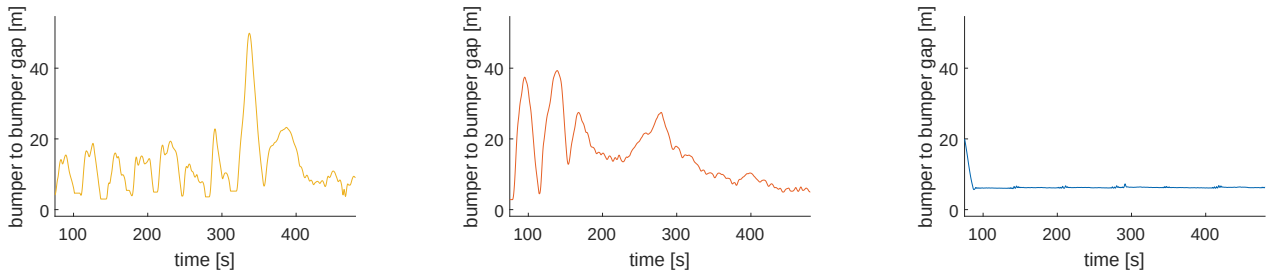

(a) Manual (b) Haptic (c) Automatic

Figure 5: Graphs of the bumper to bumper gap between the ego vehicle and the leading vehicle over time for participant 26 for each condition.

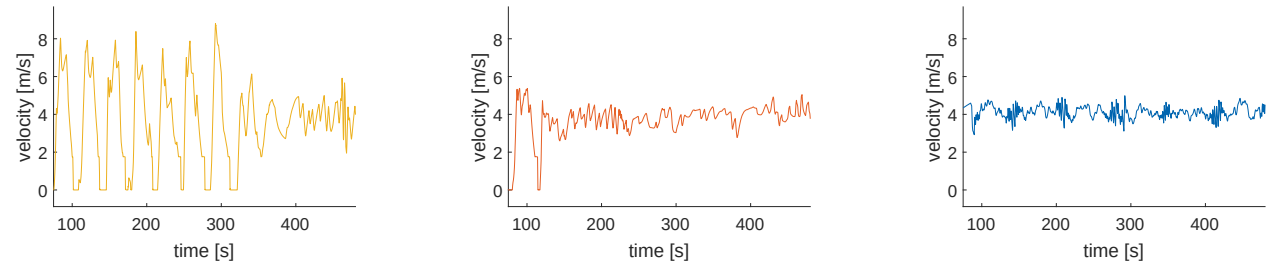

(a) Manual (b) Haptic (c) Automated

Figure 6: Graphs of the velocity of the ego vehicle over time for each condition.

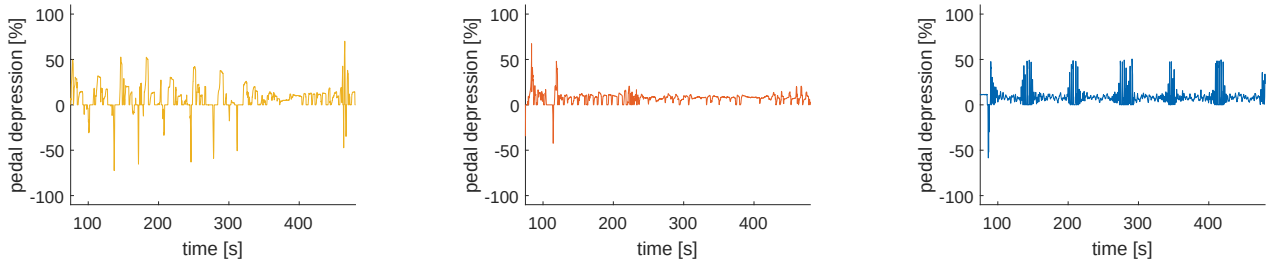

(a) Manual (b) Haptic (c) Automated

Figure 7: Graphs of the input signal of the ego vehicle over time for each condition. positive values correspond to accelerator pedal depression while negative values correspond to brake pedal depression.

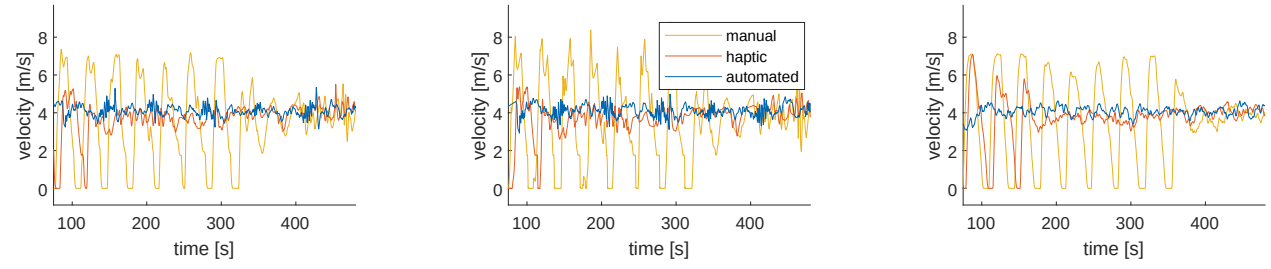

(a) Following (b) Ego (c) Leading

Figure 8: Graphs of the velocity signals for each condition for the following, ego and leading vehicle.

can be found in appendix D.

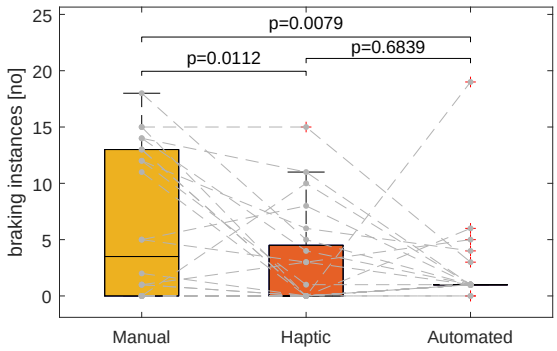

Figure 9: Number of braking instances of the ego vehicle for each condition.

TRAFFIC JAM DISSIPATION PERFORMANCE

T-tests point out that there is a significant decrease in standard deviation of the ego vehicle when comparing haptic shared control with manual control ($p = 0.0379 \quad t = 2.2028$), and automation shows a further decrease ($p = 0.0001 \quad t = 4.8916$ and $p = 0.00260 \quad t = 3.3727$ for comparing against the manual and haptic case respectively). A figure of this is shown in appendix C. Figure 9 shows the amount of braking instances for every participant for every condition. In the manual case, there are more braking instances than in the haptic and automated cases. T-tests confirm that haptic shared control as well as automation reduce the amount of braking instances significantly compared to the manual case ($p = 0.0112 \quad t = 2.7550$, and $p = 0.0079 \quad t = 2.9061$, for haptic shared control and automation respectively). However, there is no statistical evidence that automation reduces the amount of braking instances compared to haptic shared control ($p = 0.6839 \quad t = 0.4123$).

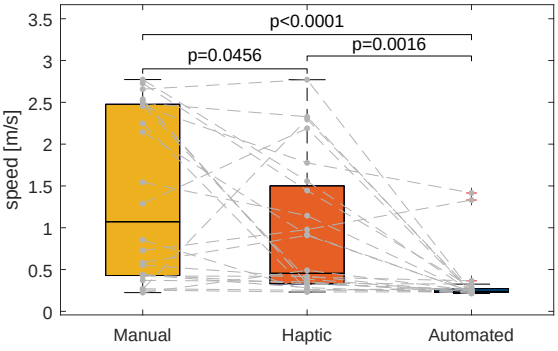

Figure 10: Standard deviation of the speed of the vehicles for the three different conditions

The influence of the different controllers on the velocity of all the cars in the flow can be seen in figure 10, where the standard deviation of the speed of all the vehicles is plotted. This figure shows that haptic shared control reduces the standard deviation of the speed for the entire flow significantly compared to the manual condition ($p = 0.0456 \quad t = 2.1128$) and automation reduces it even further compared to both the haptic shared control as well as the manual case ($p = 0.0016 \quad t = 3.5731$ and $p < 0.0001 \quad t = 4.9012$ respectively).

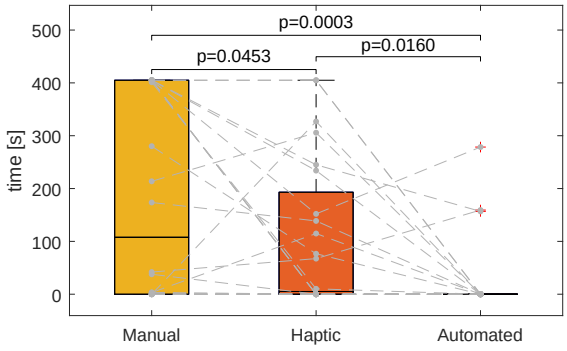

Figure 11: Lifetime of the stop and go wave for the three conditions

A boxplot of the traffic jam lifetime is shown in figure 11. T-tests confirm a significant decrease in lifetime when comparing the haptic case with the manual case ($p = 0.0453 \quad t = 2.116$), and when comparing the automated case with the manual case and the haptic shared control case ($p = 0.0003 \quad t = 4.1849$ and $p = 0.0160 \quad t = 2.5985$ respectively). In the manual control case, in 9 out of 24 cases the jam was not solved, and in the haptic shared control case, it was not solved in 2 out of 24 cases. In the automatic case, the jam was always solved. McNemar tests point out that, for the amount of traffic jams solved, a significant difference is found when comparing haptic shared control with manual control ($Mcnemar \quad \chi^2 = 5.143, p = 0.02334$), and comparing automation with manual control ($Mcnemar \quad \chi^2 = 7.111, p = 0.007661$). There is no proof of a significant difference when comparing haptic shared control with automation ($Mcnemar \quad \chi^2 = 0.5, p = 0.4795$).

Figure 12 shows the throughput in vehicles per minute for all three conditions. The throughput for the manual and haptic shared control case are in the same range, both in terms of median and variance. A t-test confirms this ($p = 0.9327 \quad t = 0.0853$). The throughput for the automated condition is higher than the manual and haptic case. A t-test confirms this ($p = 0.0002 \quad t = 4.3711$ and $p < 0.0001 \quad t = 4.8840$ for comparing automation against the haptic and manual case respectively). The other travel time metric, mean speed, shows similar results. Here, as with the throughput, there is no significant difference found between the haptic shared control case and the manual case ($p = 0.0972 \quad t = 1.7289$), but automation does increase the mean speed significantly ($p < 0.0001 \quad t = 6.0213$ and

$p < 0.0001 \quad t = 7.5112$ compared against the haptic and manual case respectively). A boxplot of the mean speed is shown in appendix C.

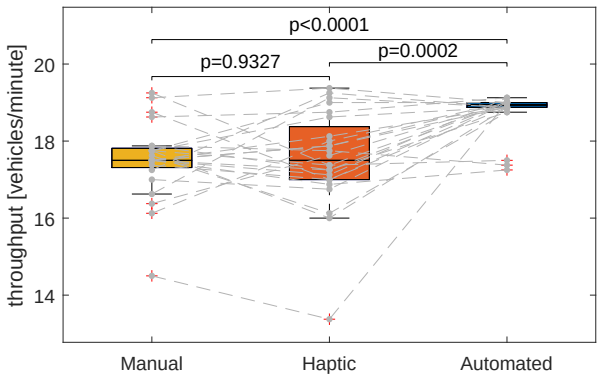

Figure 12: Throughput of vehicles during the three different conditions

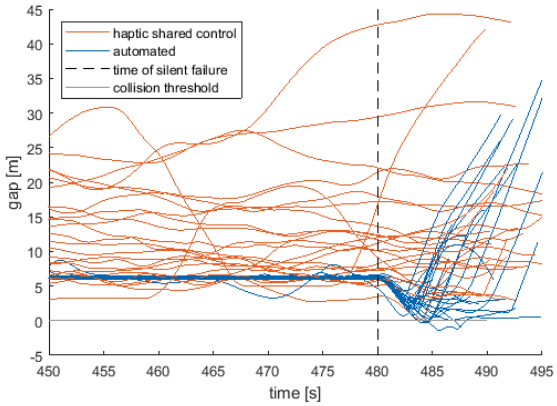

Figure 13: Bumper to bumper gap between the ego vehicle and the leading vehicle from 450s until the end of the run for the haptic shared control and automated conditions

SAFETY

Figure 13 shows the bumper to bumper gap between the ego and leading vehicle starting thirty seconds before the automation failure, until the end of each experiment for the haptic and automated condition. When the silent failure occurs at 480 seconds, the automation algorithm depresses the accelerator pedal, which speeds up the car, shortening the gap. To avoid a collision, the driver needs to intervene and press the brake, after which the gap increases again. This is shown in the blue lines in figure 13. In 5 out of 24 experiments, this automation failure caused the gap value to drop below 0, which means that, in a real life scenario, a collision would have happened. For the haptic controller, in some of the cases the gap reduces after the silent failure, but this reduction is never as drastic as in the automated case and values below 0 are never reached. This finding is illustrated in figure 14, which shows the minimal value the gap signal reaches after 480 seconds.

The increase in minimal gap size for the haptic condition compared to the automatic condition is also shown to be significant with a t-test ($p < 0.0001 \quad t = 5.3917$). The collision occurrence is also compared between the haptic and automated case. However, the McNemar test does not report a significant decrease in the amount of collisions ($Mcnemar \quad \chi^2 = 3.2, p = 0.073638$).

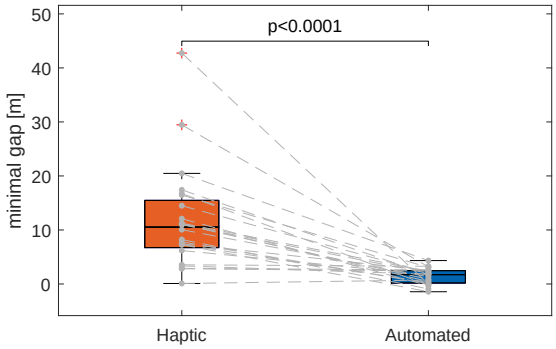

Figure 14: Minimal bumper to bumper gap for the haptic and automated condition after the silent failure, for all the participants

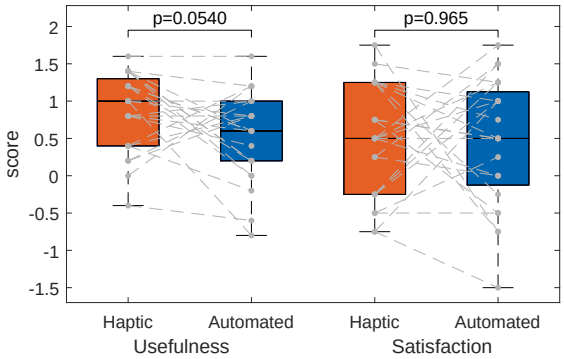

Figure 15: Acceptance scores for the haptic shared control system and the automated system

ACCEPTANCE SCORES

The Van der Laan acceptance scores are shown in figure 15. As the figure shows, the scores of the haptic shared control and automated condition, lie close together. This observation is confirmed by the statistical t-test for the usefulness ($p = 0.0541, t = 2.030$) and satisfaction ($p = 0.9650, t = 0.044$). This means that there is no statistical proof of an increase or decrease in acceptance for the haptic shared control system compared to the full automation case. However, what can be seen when looking at the grey lines in figure 15 that combine the points that belong to the same participant, is that 43 out of 48 lines are skewed, meaning that the same mean score for the haptic and automated condition is a result of the fact that the majority of participants prefer one system over the other, but the preferred system changes per participant.

IV. DISCUSSION

The results from the previous section show how haptic shared control stabilises traffic and dissipates stop and go waves both sooner and more often than manual control. However, there is no statistical evidence that haptic shared control results in improved mean speed or vehicle throughput. Full automation increases stability and jam dissipation as well as mean speed and vehicle throughput. This increase is significant compared to manual control as well as haptic shared control. After the silent automation failure, no collisions are caused in the haptic shared control condition, while in the automatic case, a collision happened five times. This result is not significant, but the decrease in the minimal gap value that automation causes compared to the haptic case is. As for the van der Laan acceptance scores, there is no proof of a significant difference between the usefulness and satisfaction scores of the haptic and automatic systems.

The improved performance and stability that the automation achieves over the manual control case are in line with the findings by Stern et al. (2018), which evaluated the same ring road scenario. An important note is that Stern et al. (2018) managed to obtain much higher mean speeds (about 7.5 m/s) than are obtained in our study (not higher than 4 m/s). This difference could have happened because Stern et al. (2018) instructed the human drivers to keep a much smaller gap than they would normally do. We did not instruct the simulated human drivers in this study to keep a tight gap because this is not in line with the driving behaviour of regular human drivers. The fact that the achieved dissipation performance of the haptic shared controller lies between the manual control case and the automated case is in line with our hypotheses. It is also in line with the essence of haptic shared control to share manual control with automation. While the jam dissipation improves for haptic shared control, the mean speed and throughput do not. This result is not in line with publications about traffic stability and throughput (Tadaki et al. (2013)) but could have happened due to the low driving speeds in this particular driving scenario. Because of the slow driving speeds, bringing the car to a stop and speeding it up takes less time than in a simulation where realistic highway speeds are tested. The result from the silent automation failure that causes collisions in the automated case results in a higher bumper-to-bumper in the haptic case is in line with publications about vigilance decrement and increased reaction times (Parasuraman (1987),Rudin-Brown and Parker (2004)). This result also corresponds with the study from Flemisch et al. (2008), which evaluated a similar scenario for haptic shared control for lateral vehicle motion to illustrate the advantage of keeping the driver in the loop.

As we stated in the introduction, the main problems that phantom traffic jams cause are increased travel times, fuel consumption and crashes. The results show that travel time is not improved with haptic shared control compared to the manual case, although it is also not decreased. Automation decreases travel time compared to manual control. The fuel consumption of the cars is difficult to compare because this depends on many factors. The best measure that represents fuel consumption is the standard deviation of the speed and braking instances. When these metrics are relatively high, the vehicles speed up and slow down often. These velocity oscillations cost mechanical energy for which the cars consume fuel. The haptic shared controller would then significantly reduce fuel consumption, but automation reduces it even further. We compared the number of crashes directly in the result section. There is no proof of a significant decrease in collisions when comparing haptic shared control with automation. However, there is a significant decrease in the minimal gap size between the ego vehicle and the leading vehicle, making it easier for vehicles to collide.

The controller that calculates the ideal pedal position shows oscillatory behaviour in the input signal in figure 7c. Even when there is no phantom traffic jam, the accelerator pedal moves aggressively compared to the haptic and manual case. This behaviour is a thing that we overlooked when tuning the traffic controller. We tuned the controller to solve the phantom traffic jam, not to minimise the accelerator input. This pedal behaviour results in a velocity that oscillates more heavily than that of the haptic shared control case when the phantom traffic jam is solved. As figures 5c, 6c and 7c show, the input and velocity oscillate to keep the gap value constant. This is not be the ideal way to control a vehicle because **1):** it would make the controller less desirable because a car with an oscillating velocity is not comfortable to drive in and **2):** it would contribute to one of the problems associated with phantom traffic jams, fuel consumption. We, therefore, recommend that future studies that aim to stabilise phantom traffic jams tune the controller to improve both the phantom traffic jam dissipating performance and the velocity oscillations. Another important note is that this study has only shown the efficacy of haptic shared control for an artificial ring road scenario. Although this scenario shows the theoretical promise of haptic shared control, it is unrealistic in several ways. First of all, phantom traffic jams occur on highways where cars drive at speeds in the range of 80-120 km/h. In this scenario, velocities range from 0 to 20 km/h. Furthermore, the ring road itself is not a representative infrastructure of actual highways, which are usually straight and on which there is almost always more than one lane. So if we want to conclude something meaningful about the effectiveness of haptic shared control for dissipating phantom traffic jams, this controller would have to be evaluated in more realistic scenarios. For example, a simulation of a stretch of highway that directly monitors travel time and fuel consumption would gain an accurate insight into the influence of haptic shared control on the consequences of phantom traffic jams.

This research is the first to combine haptic shared control with dissipating phantom traffic jams, but it will not be the last if we want to gain better insight into the effectiveness of this means of traffic control.

V. CONCLUSION

For this research, we performed driving tests in a fixed-base simulator to evaluate the efficacy of haptic shared control to dissipate phantom traffic jams. We hypothesized that haptic shared control would increase traffic jam dissipation properties compared to manual control and that full automation would show a further increase. We hypothesized that haptic shared control increases the minimal gap and decreases the number of collisions in case of an automation failure.

- Haptic shared control shows improvement in traffic stability and traffic jam solve time, but not in throughput and mean speed.
- There is no significant proof of a change in throughput and mean speed compared to the manual case.
- Minimal gap size is improved compared to automation when a silent automation failure happens.

We conclude that haptic shared control shows promise for lowering the increased fuel consumption and crashes that phantom traffic jams cause. There is no proof that haptic shared control would decrease travel time, while full automation does decrease this.

REFERENCES

Abbink, D. A., & Mulder, M. (2010). Neuromuscular analysis as a guideline in designing shared control. *Advances in Haptics, Mehrdad Hosseini Zadeh (Ed.), ISBN: 9789533070933*.

Adell, E., Várhelyi, A., & Hjälmdahl, M. (2008). Auditory and haptic systems for in-car speed management–a comparative real life study. *Transportation research part F: traffic psychology and behaviour*, *11*(6), 445–458.

Azzi, S., Reymond, G., Mérienne, F., & Kemeny, A. (2011). Eco-driving performance assessment with in-car visual and haptic feedback assistance. *Journal of Computing and Information Science in Engineering*, *11*(4).

Bainbridge, L. (1983). Ironies of automation. *Analysis, design and evaluation of man–machine systems* (pp. 129–135). Elsevier.

Čičić, M., & Johansson, K. H. (2018). Traffic regulation via individually controlled automated vehicles: A cell transmission model approach. *2018 21st International Conference on Intelligent Transportation Systems (ITSC)*, 766–771.

Flemisch, F., Kelsch, J., Löper, C., Schieben, A., Schindler, J., & Heesen, M. (2008). Cooperative control and active interfaces for vehicle assitsance and automation.

Goldmann, K., & Sieg, G. (2020). Economic implications of phantom traffic jams: Evidence from traffic experiments. *Transportation Letters*, *12*(6), 386–390.

Gunter, G., Gloudemans, D., Stern, R. E., McQuade, S., Bhadani, R., Bunting, M., Delle Monache, M. L., Lysecky, R., Seibold, B., Sprinkle, J., et al. (2020). Are commercially implemented adaptive cruise control systems string stable? *IEEE Transactions on Intelligent Transportation Systems*.

Hoogendoorn, S., Daamen, W., Hoogendoorn, R., & Goemans, J. (2013). Assessment of dynamic speed limits on freeway a20 near rotterdam, netherlands. *Transportation research record*, *2380*(1), 61–71.

Jamson, A., Hibberd, D. L., & Merat, N. (2013). The design of haptic gas pedal feedback to support eco-driving. *Proceedings of the Seventh International Driving Symposium on Human Factors in Driver Assessment, Training, and Vehicle Design*, 264–270.

Jiang, J., Astolfi, A., & Parisini, T. (2021). Robust traffic wave damping via shared control. *Transportation Research Part C: Emerging Technologies*, *128*, 103110.

Kim, J., Jeong, J., Jhang, K.-y., & Park, J.-h. (2015). Demonstration of disturbance propagation and amplification in car-following situation for enhancement of vehicle platoon system. *2015 IEEE Intelligent Vehicles Symposium (IV)*, 999–1005.

Kreidieh, A. R., Wu, C., & Bayen, A. M. (2018). Dissipating stop-and-go waves in closed and open networks via deep reinforcement learning. *2018 21st International Conference on Intelligent Transportation Systems (ITSC)*, 1475–1480.

Lee, J., & Kim, J. H. (2019). Phantom traffic: Platoon formed at low traffic density. *Journal of Transportation Engineering, Part A: Systems*, *145*(2), 04018082.

Mahmud, K., Gope, K., & Chowdhury, S. M. R. (2012). Possible causes & solutions of traffic jam and their impact on the economy of dhaka city. *J. Mgmt. & Sustainability*, *2*, 112.

McNemar, Q. (1947). Note on the sampling error of the difference between correlated proportions or percentages. *Psychometrika*, *12*(2), 153–157.

Mulder, M., Abbink, D. A., Van Paassen, M. M., & Mulder, M. (2010). Design of a haptic gas pedal for active car-following support. *IEEE Transactions on Intelligent Transportation Systems*, *12*(1), 268–279.

Mulder, M., Mulder, M., Van Paassen, M., & Abbink, D. (2008). Haptic gas pedal feedback. *Ergonomics*, *51*(11), 1710–1720.

Nilsson, L. (1996). *Safety effects of adaptive cruise controls in critical traffic situations*. Statens väg-och transportforskningsinstitut., VTI särtryck 265.

Parasuraman, R. (1987). Human-computer monitoring. *Human Factors*, *29*(6), 695–706.

Rudin-Brown, C. M., & Parker, H. A. (2004). Behavioural adaptation to adaptive cruise control (acc): Implications for preventive strategies. *Transportation Research Part F: Traffic Psychology and Behaviour*, *7*(2), 59–76.

Son, B., Kim, T., & Shin, Y. (2006). A solution for the dropout problem in adaptive cruise control range sensors. *International Conference on Embedded and Ubiquitous Computing*, 979–987.

Stern, R. E., Cui, S., Delle Monache, M. L., Bhadani, R., Bunting, M., Churchill, M., Hamilton, N., Pohlmann, H., Wu, F., Piccoli, B., et al. (2018). Dissipation of stop-and-go waves via control of autonomous vehicles: Field experiments. *Transportation Research Part C: Emerging Technologies*, *89*, 205–221.

Sugiyama, Y., Fukui, M., Kikuchi, M., Hasebe, K., Nakayama, A., Nishinari, K., Tadaki, S.-i., & Yukawa, S. (2008). Traffic jams without bottlenecks—experimental evidence for the physical mechanism of the formation of a jam. *New journal of physics*, *10*(3), 033001.

Tadaki, S.-i., Kikuchi, M., Fukui, M., Nakayama, A., Nishinari, K., Shibata, A., Sugiyama, Y., Yosida, T., & Yukawa, S. (2013). Phase transition in traffic jam experiment on a circuit. *New Journal of Physics*, *15*(10), 103034.

Treiber, M., & Kesting, A. (2013). Traffic flow dynamics. *Traffic Flow Dynamics: Data, Models and Simulation, Springer-Verlag Berlin Heidelberg*.

Van Der Laan, J. D., Heino, A., & De Waard, D. (1997). A simple procedure for the assessment of acceptance of advanced transport telematics. *Transportation Research Part C: Emerging Technologies*, *5*(1), 1–10.

Wismans, L. J., Suijs, L., Krol, L., & van Berkum, E. C. (2015). In-car advice to reduce negative effects of phantom traffic jams. *Transportation research record*, *2489*(1), 1–10.

Wu, F., Stern, R. E., Cui, S., Delle Monache, M. L., Bhadani, R., Bunting, M., Churchill, M., Hamilton, N., Piccoli, B., Seibold, B., et al. (2019). Tracking vehicle trajectories and fuel rates in phantom traffic jams: Methodology and data. *Transportation Research Part C: Emerging Technologies*, *99*, 82–109.

Appendix A: Traffic Controller

This appendix gives a more elaborate description of the haptic shared controller that was used for this research. For the controller, the ideal longitudinal motion that needs to be driven will have to be calculated first. Then, this motion needs to be transformed into ideal input signals. When the desired input values have been calculated, an algorithm needs to be developed that provides haptic feedback, based on these values.

1. Desired longitudinal motion

The desired longitudinal motion is being calculated during the simulation according to the follower stopper algorithm from Stern et al. (2018). This algorithm calculates the desired speed during the simulation. The inputs of the algorithm are a speed limit, the velocities of the ego vehicle and the leading vehicle and the gap between them. If the gap between the vehicles is large enough, the ideal speed can be driven, but as the ego vehicle closes in, the desired speed reduces to ensure the safety of the cars in the simulation. The following equations are used to calculate the desired speed:

$$v^{cmd} = \begin{cases} 0 & \text{if} \quad \Delta x \leq \Delta x_1 \\ v\frac{\Delta x - \Delta x_1}{\Delta x_2 - \Delta x_1} & \text{if} \quad \Delta x_1 < \Delta x \leq \Delta x_2 \\ v + (U - v)\frac{\Delta x - \Delta x_2}{\Delta x_3 - \Delta x_2} & \text{if} \quad \Delta x_2 < \Delta x \leq \Delta x_3 \\ U & \text{if} \quad \Delta x_3 < \Delta x \end{cases} \tag{4}$$

where

$$\Delta x_k = \Delta x_k^0 + \frac{1}{2d_k}(\Delta v\_)^2, \quad \text{for} \quad k = 1, 2, 3 \tag{5}$$

In these equations, v^{cmd} is the demanded speed, U is the maximum speed or speed limit on the road, Δx is the bumper to bumper gap between the ego and leading vehicle, v is the current speed and $\Delta v\_$ is the difference in longitudinal velocity between the ego and leading vehicle. Δx_k^0 and d_k are constant parameters, directly taken from Stern et al. (2018): $\Delta x_1^0 = 4.5m$, $\Delta x_2^0 = 5.25m$, $\Delta x_2^0 = 6.0m$, $d_1 = 1.5\frac{m}{s^2}$, $d_2 = 1\frac{m}{s^2}$ and $d_3 = 0.5\frac{m}{s^2}$. As equation 1 shows, the calculated velocity is either 0, a fraction of the current velocity, the current velocity with added to it a fraction of the difference between the current velocity and the maximum velocity or the maximum velocity. What determines v^{cmd} is based on the gap, Δx and Δx_k, of which the value depends on a certain base gap, Δx_k^0 with an added term based on the velocity difference between the two vehicles, $\Delta v\_$. A more detailed description of this algorithm can be found in Stern et al. (2018). To calculate the v^{cmd} during the simulations, a matlab function is written that takes the ego vehicle speed, leading vehicle speed, gap and speed limit as inputs. The produced v^{cmd} is then used to calculate the ideal pedal positions.

2. Ideal pedal values

To calculate the control inputs that make the vehicle reach the commanded speed, a controller is needed. The basic structure for this controller is also taken from Stern et al. (2018). This architecture is then tuned to stabilize the traffic in the simulated environment. The input for the controller is the difference between the desired speed and the current speed and the outputs are a brake and accelerator pedal position. The controller is based on the three actions that a driver can take: press the accelerator pedal, press the brake pedal or do nothing. The accelerator is pressed when the desired speed is higher than the current speed. The brake pedal is pressed when the desired speed is more than 0.25 m/s lower than the current speed. When the speed difference is between 0 and -0.25 m/s, no pedal is pressed. This corresponds to engine braking and is implemented to ensure some hysteresis which will make sure no oscillatory driving behaviour is implemented. To implement this control structure in simulink, switching logic is applied. A screenshot of the switching logic layout in simulink can be seen in figure 16. The switch passes the speed difference through to the brake and a 0 to the accelerator when a braking action needs to happen and vice versa when the car needs to accelerate. Between 0 and -0.25 m/s, a 0 is passed through to both pedals.

The control signals are not directly used as pedal inputs, but are passed trough a PID controller first. Different controllers are used for accelerating and braking. The gains used in the final simulation are displayed in table

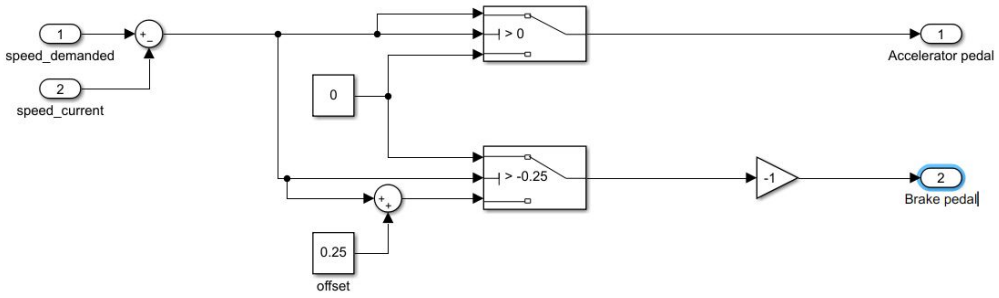

Figure 16: Snapshot of the switching logic blocks in the simulink environment

Gain	Accelerator controller	Braking controller
K_p	1	0.7
K_i	0.01	-0.04
K_d	0.05	0.1

Table 1: Control gains for the Accelerator and Braking controller

Furthermore, anti windup is enabled in both PID controllers to make sure the integral terms of the controllers don't blow up the pedal position and to make sure the values that are outputted stay between 0 and 1, because the IPG carmaker software that takes the pedal values as inputs in a range from 0 (no depression) to 1 (fully depressed). The controllers are evaluated by giving a step signal as a change in the desired speed, and then running the IPG carmaker simulation with this.

3. Pedal actuation

When the ideal pedal positions have been calculated, they need to be transformed into pedal actions. To explain this, the pedal behaviour itself must first be elaborated on. As will be explained in appendix B, the pedals consist of control loading systems. The forces that the pedals exert on the foot of the driver can be set with the software form E2M commander. For uncontrolled pedals, forces that get exerted are determined by multiplying the pedal position with a stiffness and the pedal speed with a damping term. A graphical representation of this can be seen in figure 17.

For the haptic case, the baseline behaviour of the pedals is the same in terms of stiffness and damping. However, in this controller, the stiffness of the pedals can be modified to give the driver suggestions about the ideal pedal positions. A graphical representation of this can be seen in figure 18, where the difference between the current pedal position and the ideal pedal position is multiplied by an additional stiffness K^h, which is then

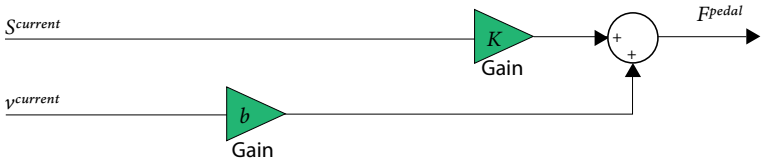

Figure 17: Schematic representation of the pedal behaviour

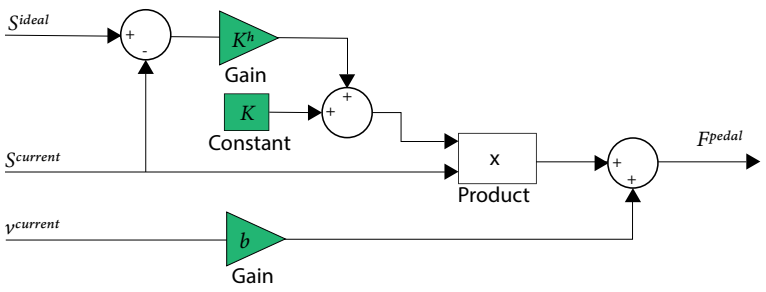

Figure 18: Schematic representation of the pedal behaviour with haptic shared control

added to the base stiffness K. Based on pilot studies, the choice was made to only provide haptic feedback on the accelerator pedal and not on the brake pedal. Also, the additional haptic stiffness was set much higher for when the pedal needed to be released than for when the pedal needed to be depressed.

For the automatic condition, the difference in current and ideal pedal position was multiplied with an additional stiffness K^a, which was then added to the force F^{pedal} to force the pedal in the ideal position. For the automatic case, both the accelerator pedal and the brake were automated.

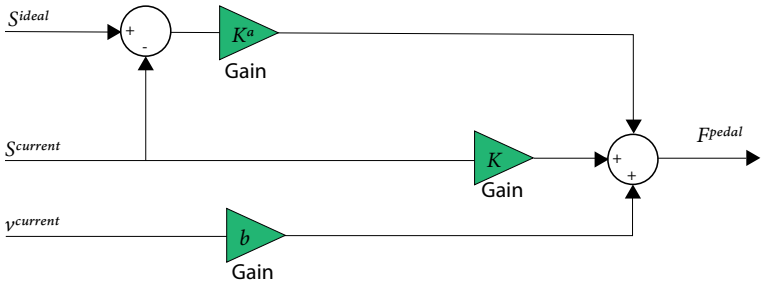

Figure 19: Schematic representation of the pedal behaviour with full automation

Appendix B: Simulator Setup

The company Cruden specializes in developing driving simulators. Because there is a demand from the car manufacturing industry for active pedals, it was possible to do this graduation project at Cruden. For this project, a simulator with an active accelerator and brake pedal were developed. This appendix explains how the simulator is built up in terms of hardware and software.

Hardware setup

Chair and frame setup The driving simulator, which can be seen in figure 3 is built up as follows: On a plate on the floor, a car seat is adjusted. The car seat position can be changed to make the simulator adapt to the driver. in front of the seat, an aluminum frame built out of Item profiles is joined to the plate on the floor. To this frame, a screen is mounted on which the simulation is projected to provide the driver with visual feedback. Inside the screen, there are speakers to give audio feedback to the driver. There is also a steering wheel joined to this frame. Beneath the steering wheel and the frame, the active pedals are fixed to the frame.

Active Pedal setup
The active pedals for this simulator come from an Audi car, they only consist of an accelerator and a brake pedal. This pedal box is fastened to the aluminium Item frame. The pedals are both connected to a control loading system. A control loading system is typically used in simulators to provide a driver with accurate feedback. In this setup, the control loaders consist of a large servo motor that is connected to the pedal with a crank and a shaft. Halfway the shaft, there is a load cell that registers the axial force in the shaft. A picture of the pedals can be seen in figure 2.

Both the servo motors of the control loading systems for the pedals are also fastened to the aluminum frame. The control loading systems that are used come from an old helicopter simulator. This simulator used 4 control loading systems and the system does not work unless all 4 control loaders are connected to it. Because of this, the two additional control loaders, although unused, were also fastened to the frame.

Motion cabinet
As mentioned before, each control loader contains a servo motor and a load cell. Both the servo motor and the load cell of the 4 control loaders are connected to a so called motion cabinet. This motion cabinet contains physical servo drivers that send commands to and receive signals from the servo motors. Receivers from the load cells, as well as a computer are also in the motion cabinet. Commands to the motion cabinet and signals from the motion cabinet are transmitted via an ethernet cable from the computer inside the cabinet. This ethernet cable is then connected to the switch in the computer cabinet.

Computer cabinet
The computer cabinet contains 5 computers on which the driving simulation is run. The computers are connected to each other via ethernet cables that are plugged into a so called switch. This switch is also connected to the motion cabinet. Different computers take different tasks in the simulation process: //

- The Operator pc is the computer from which the simulation is started
- The Replicator pc contains the Panthera software. All the signals are fed into this computer, and this computer outputs the audio and visual signals.
- The Master pc runs the simulation.

Software setup

Matlab/Simulink
The central piece of software in the simulator is Simulink. The simulation software is run from a Simulink

model. This makes it possible to use simulink signals as inputs for the simulation and to receive data from the simulation as simulink signals. The communication between the simulation software and Panthera also goes via Simulink. signals from the simulation are fed to a Simulink block that sends this data to Panthera. Also, data from the steering wheel is transmitted from Panthera into the Simulink environment, via which it gets put into the simulation software.

The Traffic controller (explained below) is also built into this Simulink, along with the pedal feedback system. Simulink receives signals such as speed, position ans acceleration from the control loaders and sends force inputs to the control loaders via the E2M commander software (explained below). As a baseline, regular pedal behaviour is simulated in Simulink by simulating stiffness and damping on the pedals. On top of this pedal behaviour, additional forces can be provided by the haptic controller or the automatic controller. The pedal positions that Simulink receives are fed into the simulation software as inputs. Simulink also saves data from the driver tests to the Matlab workspace from which it can be used for data analysis.

IPG Carmaker IPG Carmaker is the simulation software. In IPG Carmaker, signals from the pedals and the steering wheel are used as inputs for the driving simulation. The driving scenario is built in IPG Carmaker and the interactions between the different cars in the simulation and between the cars and the road are all simulated in this program.

Panthera
This system integration software program is developed by Cruden and integrates all software parts necessary to run a driving simulation. Panthera takes data from the cars in the simulation and renders the visual data that get transmitted to the screen. It also takes the input angle from the steering whele and transmits this to the simulation software. Panthera also distributes the simulation load to the different computers in the computer cabinet and ensures that the simulation is run in real time.

E2M Commander
E2M Commander is software developed by E2M Motion systems, the company that provides Cruden with the motion bases for its driving simulators. E2M Commander is the software that communicates with the motion cabinet. Signals from the control loaders that are connected to the pedals are received in the E2M Commander software and force inputs can be sent to the control loaders via the E2M Commander software. In typical Cruden simulation applications, E2M communicates directly with Panthera. For this application, the signals from and to the pedal get loaded into the Simulink environment, because the pedal feedback system is also built in the Simulink environment.

A graphical overview of the software architecture can be seen in figure 20.

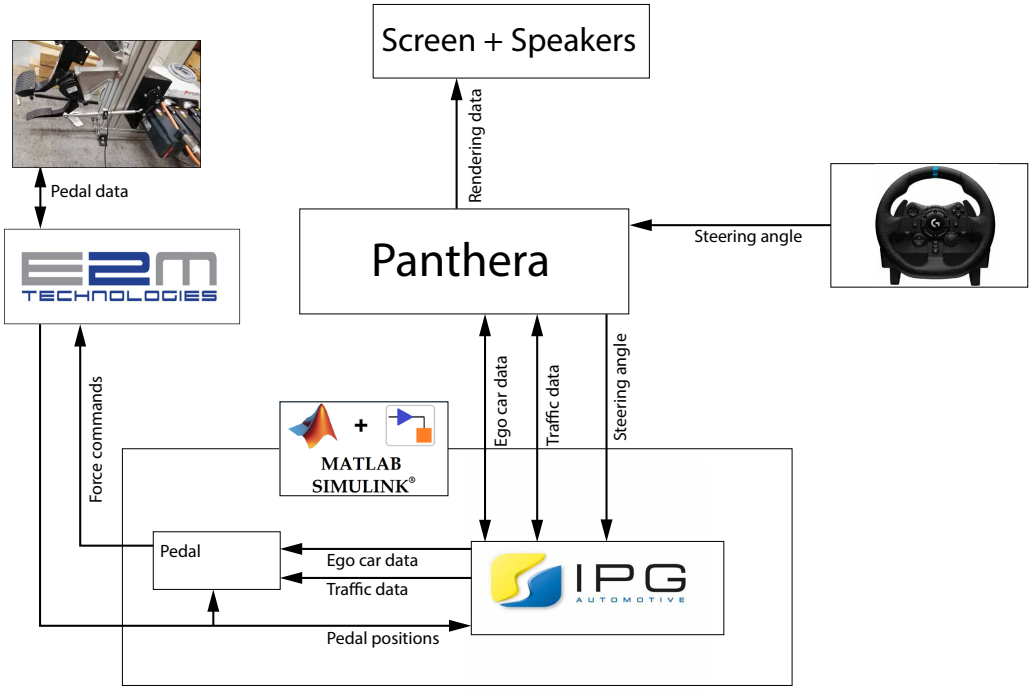

Figure 20: A graphical representation of how the different software applications communicate with each other

Appendix C: Data Analysis

This Appendix elaborates on how the data analysis was done.

Transient Behaviour

As the experiments start with the ego vehicle ahead of the 20 traffic cars that are closely spaced together, the ego vehicle needs to drive a long stretch of highway before it has entered the traffic jam once again. This means that the velocity and gap size at the start of the experiment are larger than during the rest of the experiment. To be able to analyze the data only for the time in which the participants were actually driving in the traffic jam, a point in time needed to be chosen where the initial transient behaviour had stopped. This point was determined by finding the first point in time where the gap stops to decrease. Because when the gap stops to decrease, the driver has noticed the car in front of it and this leading vehicle has started to move forward which increases the gap. The first point in time where the gap stops to decrease was found by using matlab function *findpeaks*. The highest value that was found was 70.8 seconds. Hence, the choice was made to cut the signals at 75 seconds for the data analysis of the post-transient part of the experiment. Plots of the gap values per participant are displayed in figure 21.

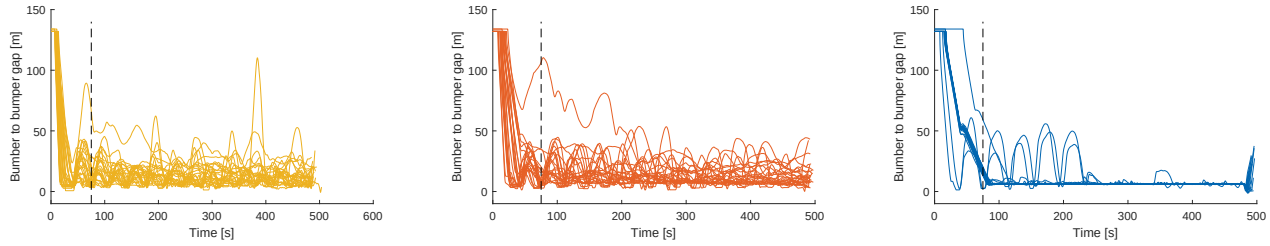

(a) manual **(b)** haptic **(c)** automatic

Figure 21: Graphs of the bumper to bumper gap between the ego vehicle and the leading vehicle over time for each vehicle for each condition

Metrics Calculations

How the raw data is transformed into metrics is described in this section.

Standard deviation ego vehicle: taking the data of the velocity of all vehicles in the flow, using the matlab function *std*, the standard deviation of the speed of all the vehicles is calculated, taking the mean of a vector containing the standard deviations of the vehicles produces the average standard deviation of the speed of all the vehicles in the simulation.

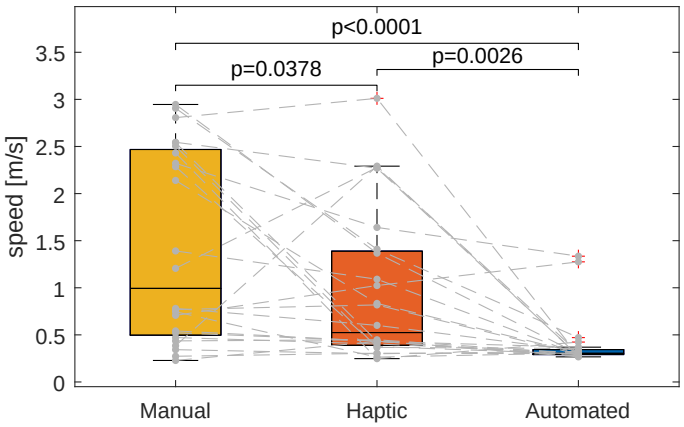

Figure 22: Boxplot of the standard deviation of the speed of the ego vehicle per condition

Number of braking instances: By loading the brake signal in matlab, smoothening the data using the matlab function *smoothdata*, and finding the peaks in this signal using the function *findpeaks*. When this was done, peaks that lay within the same 5 second range were counted as one braking instance.

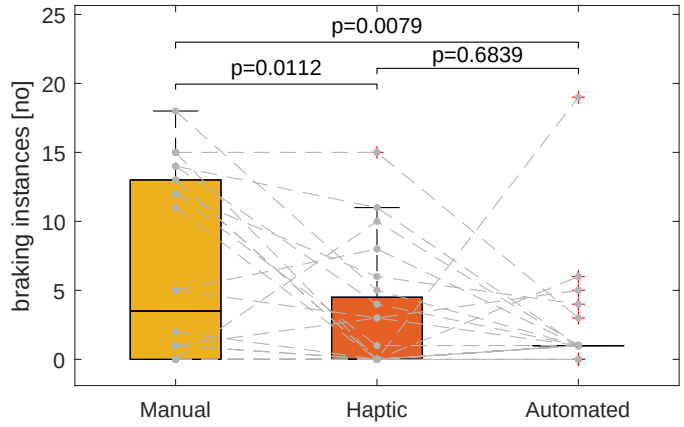

Figure 23: Boxplot of the number of braking instances per condition

Mean standard deviation: taking the data of the velocity of all vehicles in the flow, using the matlab function *std*, the standard deviation of the speed of all the vehicles is calculated, taking the mean of a vector containing the standard deviations of the vehicles produces the average standard deviation of the speed of all the vehicles in the simulation.

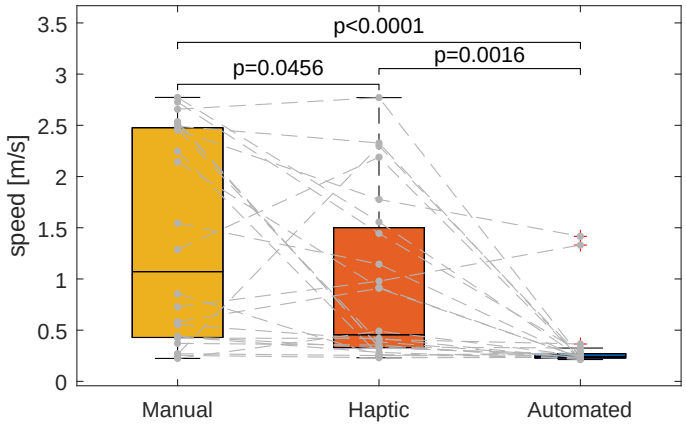

Figure 24: Boxplot of the mean standard deviation of the speed of the ego vehicle per condition

Traffic jam lifetime: by looking at what time the stop and go wave has stopped. This is done by looking at the values of the velocity signals for each individual car in the simulation, and finding the last point at which one of the vehicles stands still. When this point in time occurs before the end of the experiment, this means that form that point on, the cars do not stop anymore and the stop and go wave has been solved. When this point happens at the end of the experiment, it means that there are still one or more cars standing still

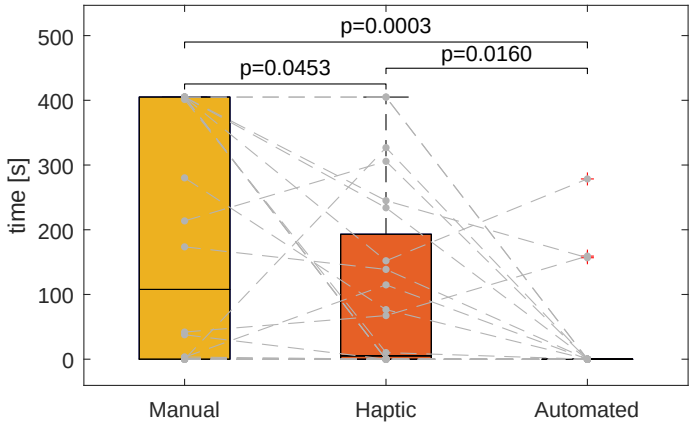

Figure 25: Boxplot of the traffic jam lifetime per condition

Throughput: Throughput is defined as the amount of vehicles that pass the origin of the ring road per minute. The ego vehicle starts at the origin of the ring road. The throughput is calculated by taking the distance that the ego vehicle has driven and dividing this by the ring road circumference. The result is the amount of rounds the ego vehicle has driven. Rounding this off using the matlab function *floor* to the largest integer beneath the calculated value produces the amount of rounds that all the cars have driven. This number is then multiplied by 21. This is added to the number of cars that have passed the origin after the ego vehicle. This number is calculated by finding the distance of the vehicle that is closest to the origin. The number that is produced is then divided by 8 to result in the amount of vehicles per minute that pass the origin on average.

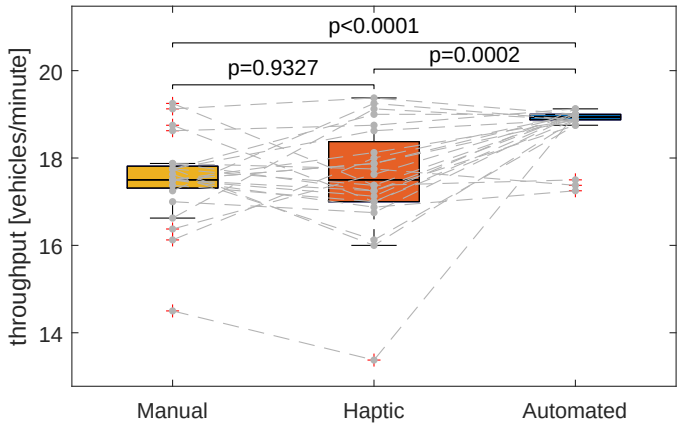

Figure 26: Boxplot of the vehicle throughput per minute per condition

Mean speed: taking the data of the velocity signals of all vehicles in the flow, using the matlab function *mean*, the mean speed of all the vehicles is calculated, taking the mean of a vector containing the mean speeds of the vehicles produces the average mean speed of all the vehicles in the simulation.

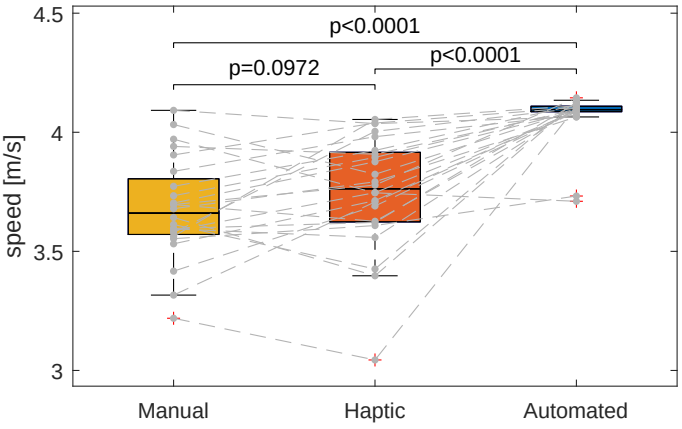

Figure 27: Boxplot of the mean speed per condition

Minimal gap: by taking the data from 480 seconds until the end of the bumper to bumper gap signal. The matlab command *min* is used to find the minimal value.

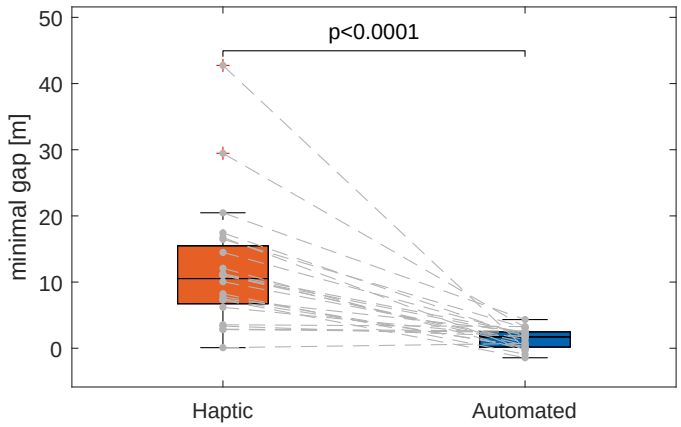

Figure 28: Boxplot of the minimal bumper to bumper gap after the automation failure for the haptic and automatic condition

Van der Laan Usefulnes and Satisfaction score: by taking the scores from the Van der Laan accpetance test, multiplying the 9x1 vector containing the scores by vector [-1;-1;1;-1;-1;1;-1;1;-1]. This is done because in the form, words that correspond to a high usefulness or acceptance are sometimes switched around to prevent people from just filling out one side of the boxes, but to make them think about each question separately. When the multiplication with the vector is done, values 1,3,5,7,9 are summed and divided by 5 to produce the usefulness score with a value between -2 and 2 and values 2,4,6,8 are added and divided by 4 to produce the satisfaction score with a value between -2 and 2.

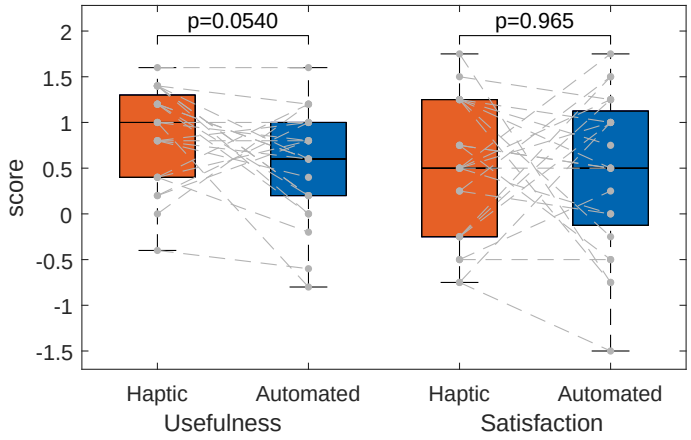

Figure 29: Boxplot of the Van der Laan usefulness and satisfaction scores for the haptic and automatic condition

Statistics

T-tests: The statistical comparison of the mean speed, standard deviation of the speed, throughput, number of braking instances, traffic jam solve time and the acceptance scores are compared by doing a t-test. The matlab function *ttest* was done to obtain the t value, the value that represents how far the two found means lie apart, and the p value, the value that represents the chance that the two vectors were drawn from the same distribution.

McNemar's tests For the comparison of the traffic jams solved and the collision occurrence, which are not values, but binary events, McNemar's test was done. This test evaluates the effect statistical significance of, for example changing the means of control from manual to haptic shared control in order to increase the amount of traffic jams that are solved. The matlab function *mcnemar* requires a 2x2 matrix as input that correspond to values (2,2),(2,3),(3,2) and (3,3) from table 2, 3, 4 and 5. The function produces the Mcnemar χ^2 value that is a measure for significance and a p-value.

	Jam Not Solved Haptic	Jam Solved Haptic	Row Total
Jam Not Solved Manual	2	7	9
Jam Solved Manual	0	15	15
Collumn Total	2	22	24

Table 2: McNemar test for the statistical comparison for the events in which the traffic jam was solved, comparing haptic shared control with manual control

McNemar $\chi^2 = 5.142857$
p = 0.023342

	Jam Not Solved Automation	Jam Solved Automation	Row Total
Jam Not Solved Haptic	0	2	2
Jam Solved Haptic	0	22	22
Collumn Total	0	24	24

Table 3: McNemar test for the statistical comparison for the events in which the traffic jam was solved, comparing haptic shared control with automation

McNemar $\chi^2 = 0.500000$
p = 0.479500

	Jam Not Solved Automation	Jam Solved Automation	Row Total
Jam Not Solved manual	0	9	9
Jam Solved manual	0	15	15
Collumn Total	0	24	24

Table 4: McNemar test for the statistical comparison for the events in which the traffic jam was solved, comparing manual control with automation

McNemar $\chi^2 = 7.111111$
p = 0.007661

	Collision Haptic	No Collision Haptic	Row Total
Collision Automation	0	5	5
No Collision Automation	0	19	19
Collumn Total	0	24	24

Table 5: McNemar test for the statistical comparison of the occurrence of collisions in the haptic shared control and automated case

McNemar $\chi^2 = 3.2$ p $= 0.073638$

Additional figures

For the data analysis. Several figures were made to gain insight in the car following during the tested scenario. First off, a scatter plot was made that displays the mean relative distance (or bumper-to-bumper gap) against the mean relative velocity. Figure 30 shows these data points. However, this figure does not give more insight than the plots of the bumper-to-bumper signals over time. It shows how the relative distance is spread out for the manual and haptic case and how the automatic case keeps this distance constant. The relative velocity is equally spread out for all three conditions.

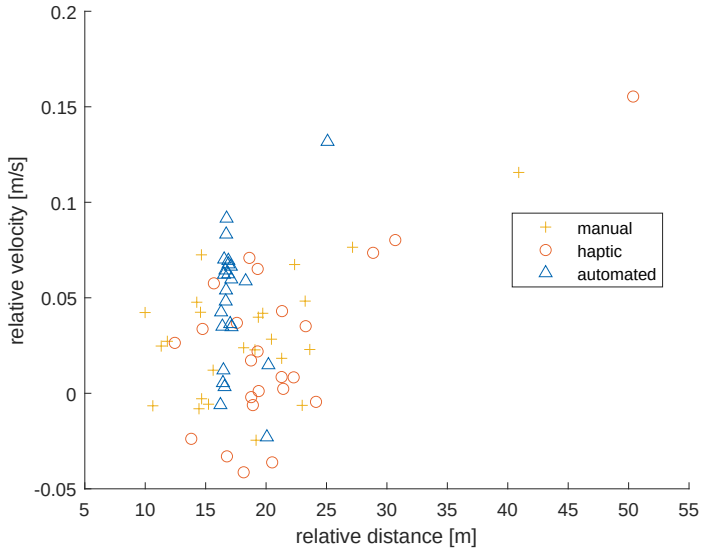

Figure 30: Scatterplot of the mean relative distance over the mean relative velocity. There is a datapoint for each participant for each condition.

A plot of the time headway and inverse time to collision was also made to gain insight into the car following behaviour. This plot can be seen in figure 31. The time headway is calculated by dividing the relative distance by the relative speed, resulting in the time the ego vehicle would need to reach the leading vehicle. The time to collision is calculated by dividing the relative distance by the relative velocity. In the car following studies such as Mulder et al (2011), a plots of these metrics showed cyclic behaviour. However, for our car following scenario, it does not. We expect that this is because of the nonlinear coupling of the longitudinal motion of all of the vehicles in the flow.

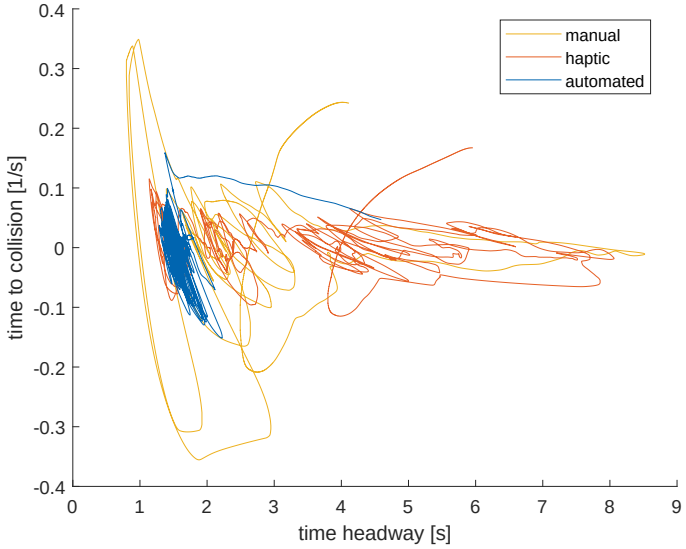

Figure 31: Time headway plotted against inverse time to collision for all conditions for participant 26.

Appendix D: Raw Data

This appendix contains the collected raw data from each participant. From the 30 driving experiments that were done, experiment 1, 2, 3, 4, 7 and 8 were deemed unuseable because of either problems with saving the data or because an older scenario was evaluated.

Participant 5

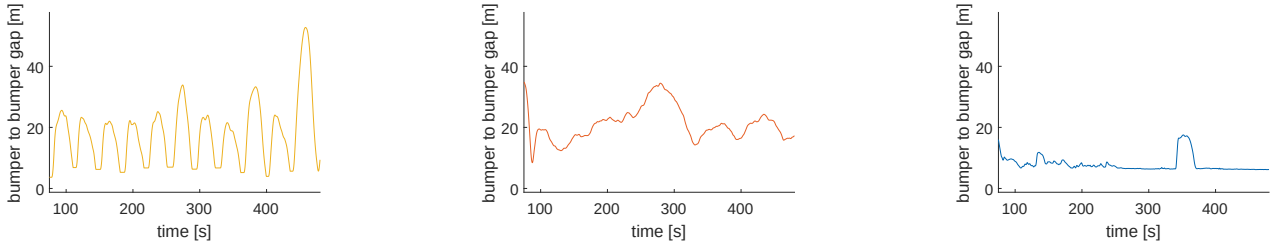

(a) manual (b) haptic (c) automatic

Figure 32: plots of the bumper to bumper gap between the ego vehicle and the leading vehicle over time for each condition

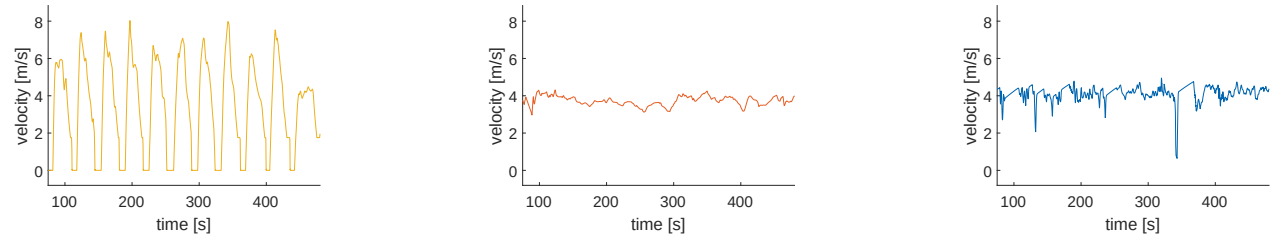

(a) manual (b) haptic (c) automated

Figure 33: plots of the velocity of the ego vehicle over time for each condition

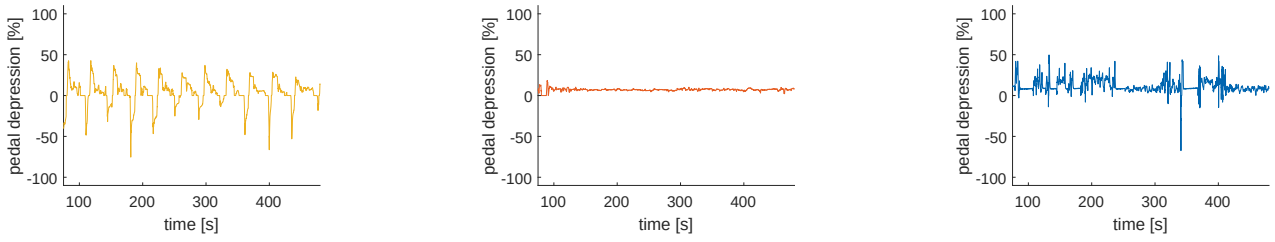

(a) manual (b) haptic (c) automated

Figure 34: plots of the pedal input of the ego vehicle over time for each condition. positive values correspond to accelerator pedal depression while negative values correspond to brake pedal depression

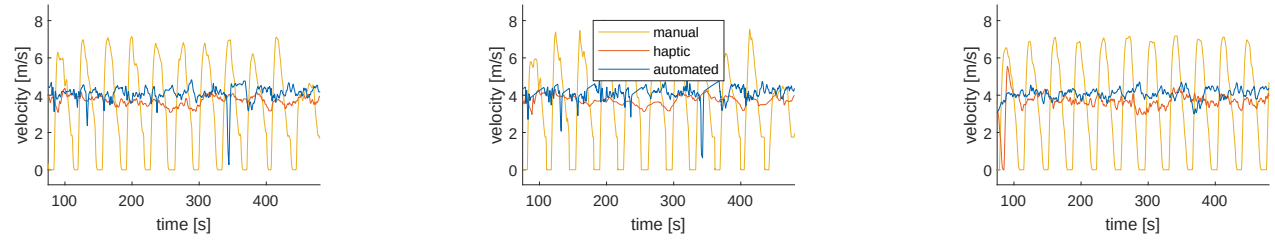

(a) following (b) ego (c) leading

Figure 35: plots of the velocity over time for each condition for the following vehicle, the ego vehicle and the leading vehicle

Participant 6

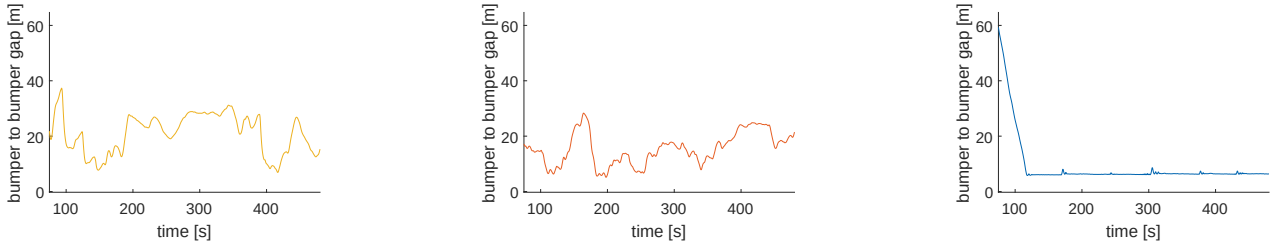

(a) manual (b) haptic (c) automatic

Figure 36: plots of the bumper to bumper gap between the ego vehicle and the leading vehicle over time for each condition

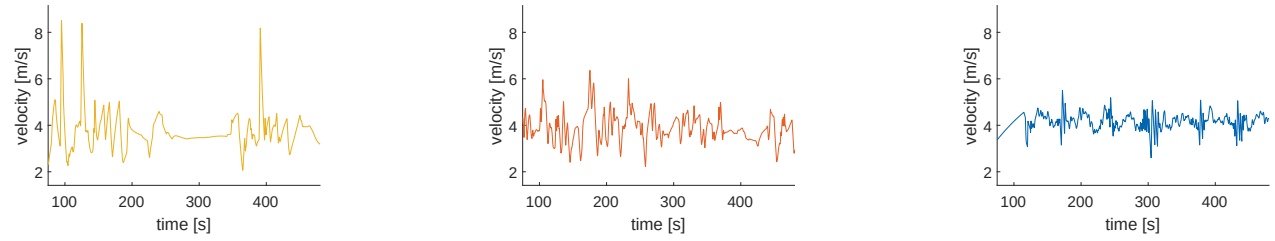

(a) manual (b) haptic (c) automated

Figure 37: plots of the velocity of the ego vehicle over time for each condition

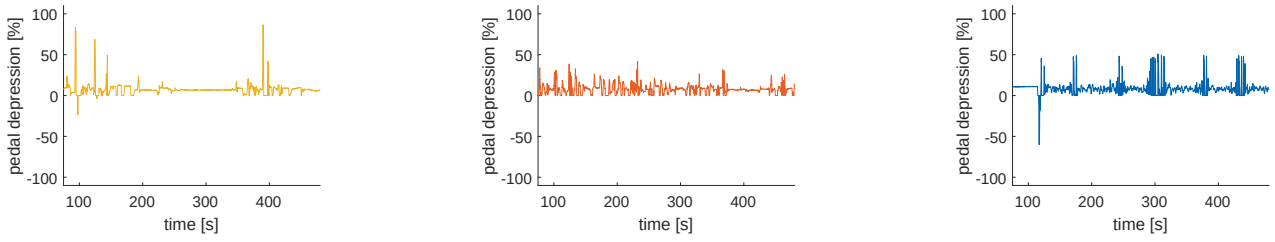

(a) manual (b) haptic (c) automated

Figure 38: plots of the pedal input of the ego vehicle over time for each condition. positive values correspond to accelerator pedal depression while negative values correspond to brake pedal depression

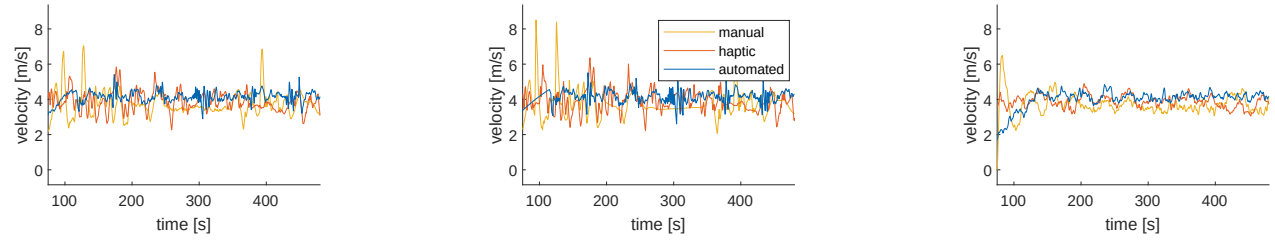

(a) following (b) ego (c) leading

Figure 39: plots of the velocity over time for each condition for the following vehicle, the ego vehicle and the leading vehicle

Participant 9

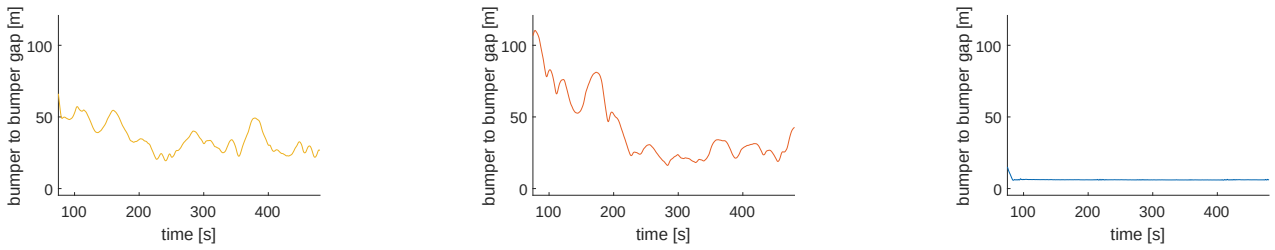

(a) manual (b) haptic (c) automatic

Figure 40: plots of the bumper to bumper gap between the ego vehicle and the leading vehicle over time for each condition

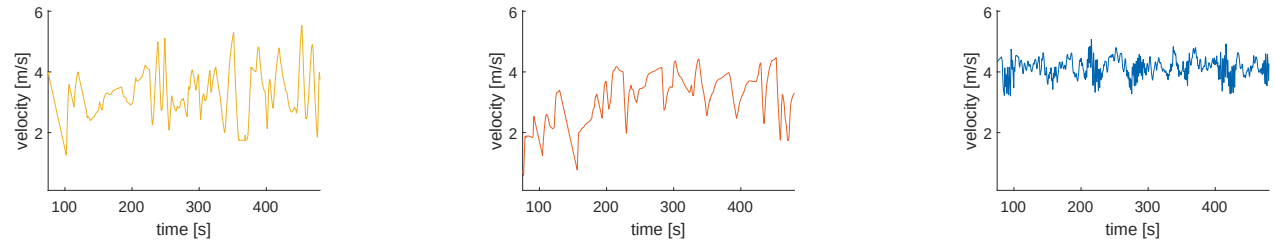

(a) manual (b) haptic (c) automated

Figure 41: plots of the velocity of the ego vehicle over time for each condition

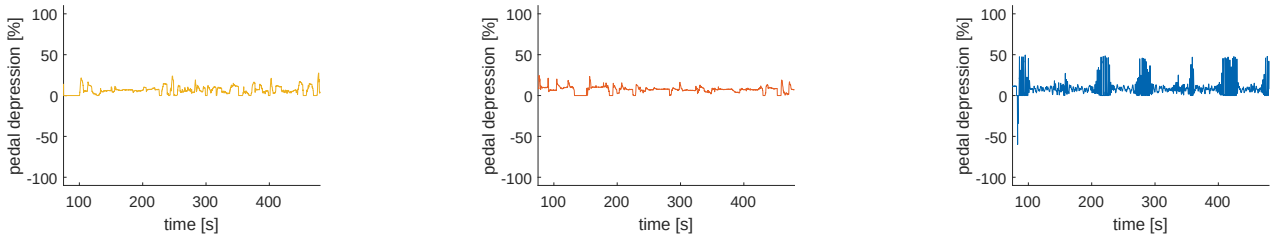

(a) manual (b) haptic (c) automated

Figure 42: plots of the pedal input of the ego vehicle over time for each condition. positive values correspond to accelerator pedal depression while negative values correspond to brake pedal depression

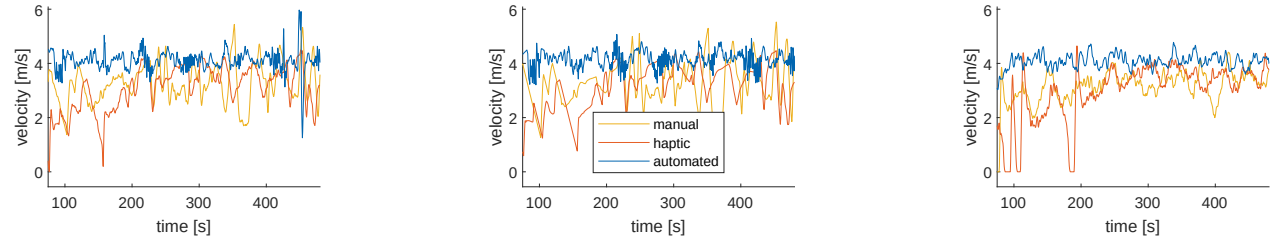

(a) following (b) ego (c) leading

Figure 43: plots of the velocity over time for each condition for the following vehicle, the ego vehicle and the leading vehicle

Participant 10

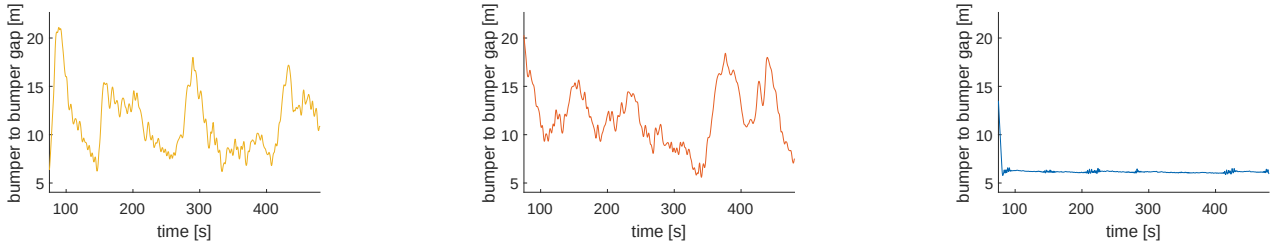

(a) manual (b) haptic (c) automatic

Figure 44: plots of the bumper to bumper gap between the ego vehicle and the leading vehicle over time for each condition

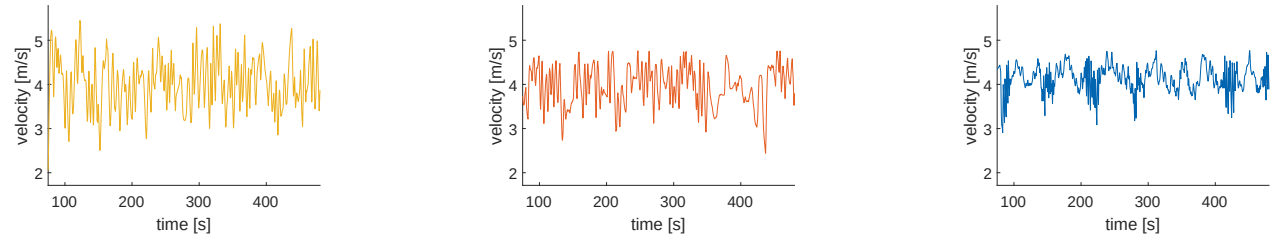

(a) manual (b) haptic (c) automated

Figure 45: plots of the velocity of the ego vehicle over time for each condition

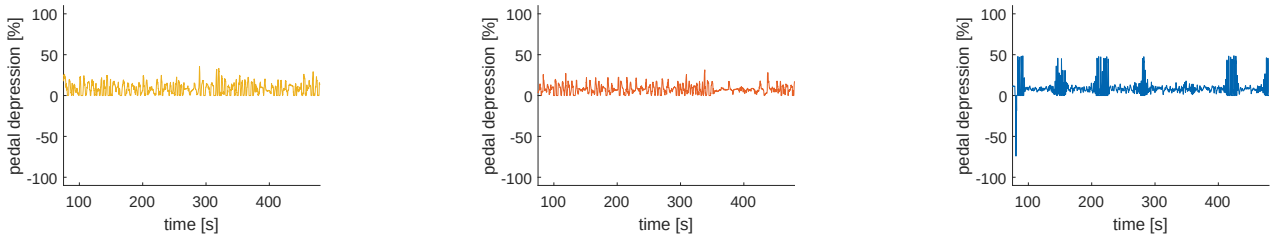

(a) manual (b) haptic (c) automated

Figure 46: plots of the pedal input of the ego vehicle over time for each condition. positive values correspond to accelerator pedal depression while negative values correspond to brake pedal depression

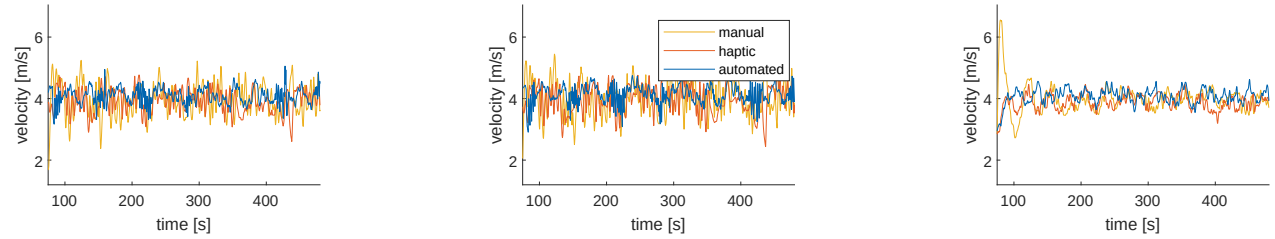

(a) following (b) ego (c) leading

Figure 47: plots of the velocity over time for each condition for the following vehicle, the ego vehicle and the leading vehicle

Participant 11

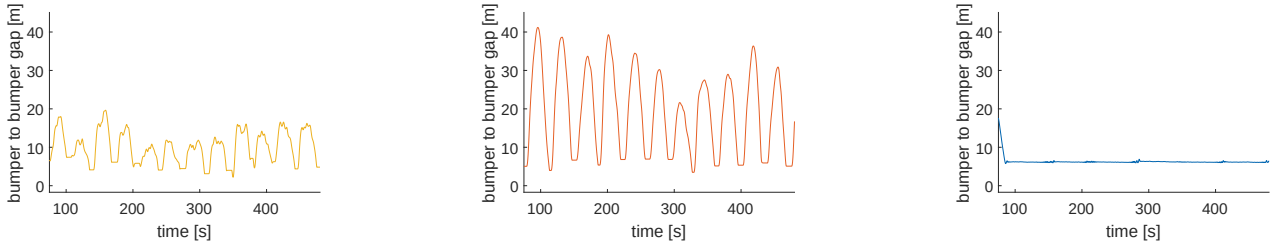

(a) manual (b) haptic (c) automatic

Figure 48: plots of the bumper to bumper gap between the ego vehicle and the leading vehicle over time for each condition

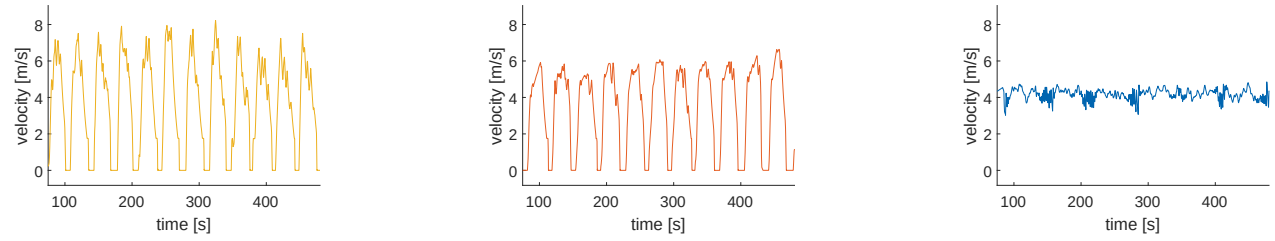

(a) manual (b) haptic (c) automated

Figure 49: plots of the velocity of the ego vehicle over time for each condition

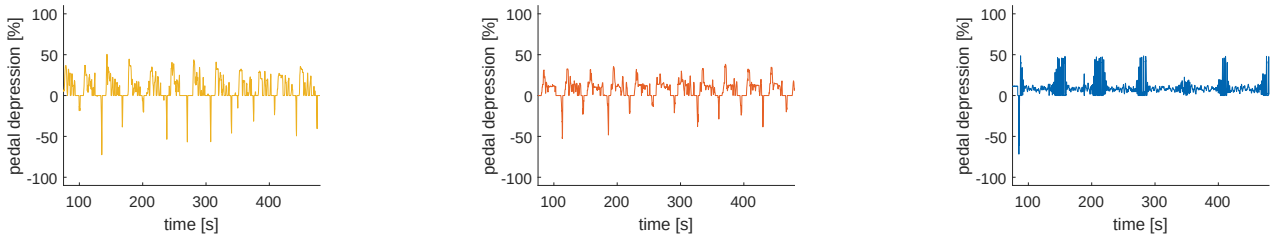

(a) manual (b) haptic (c) automated

Figure 50: plots of the pedal input of the ego vehicle over time for each condition. positive values correspond to accelerator pedal depression while negative values correspond to brake pedal depression

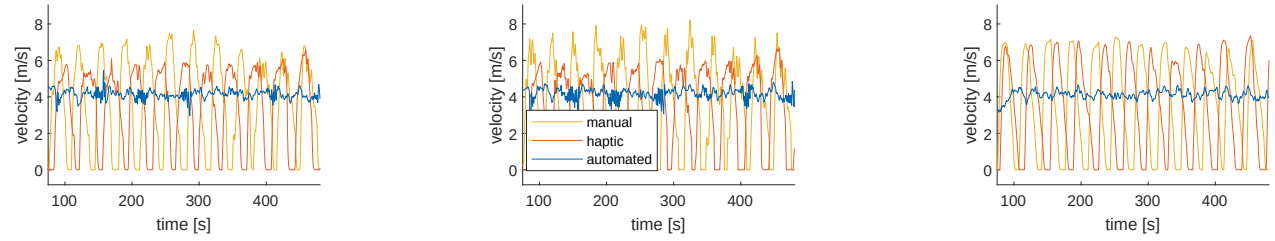

(a) following (b) ego (c) leading

Figure 51: plots of the velocity over time for each condition for the following vehicle, the ego vehicle and the leading vehicle

Participant 12

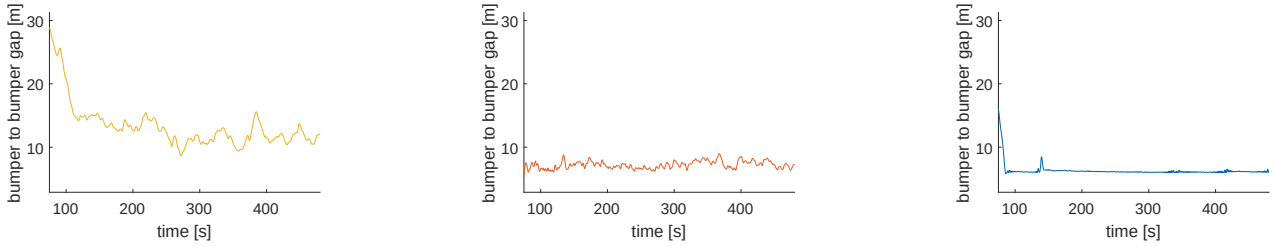

(a) manual (b) haptic (c) automatic

Figure 52: plots of the bumper to bumper gap between the ego vehicle and the leading vehicle over time for each condition

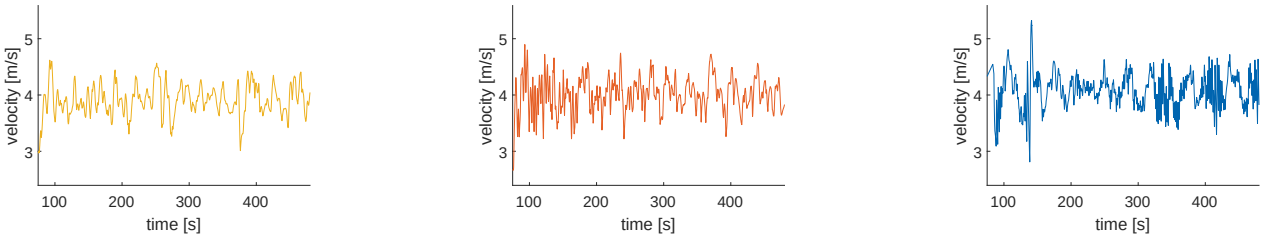

(a) manual (b) haptic (c) automated

Figure 53: plots of the velocity of the ego vehicle over time for each condition

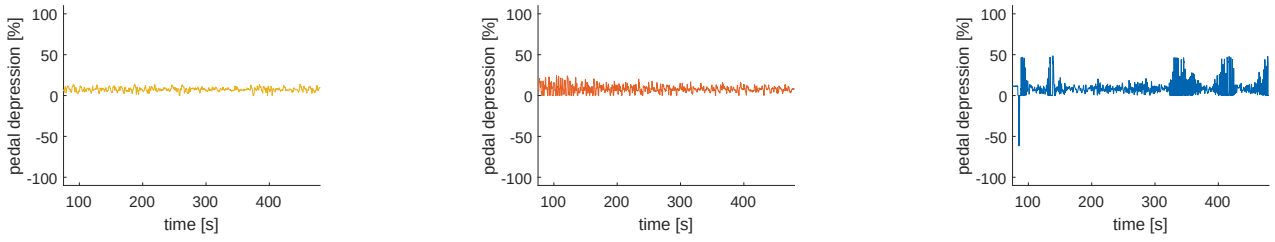

(a) manual (b) haptic (c) automated

Figure 54: plots of the pedal input of the ego vehicle over time for each condition. positive values correspond to accelerator pedal depression while negative values correspond to brake pedal depression

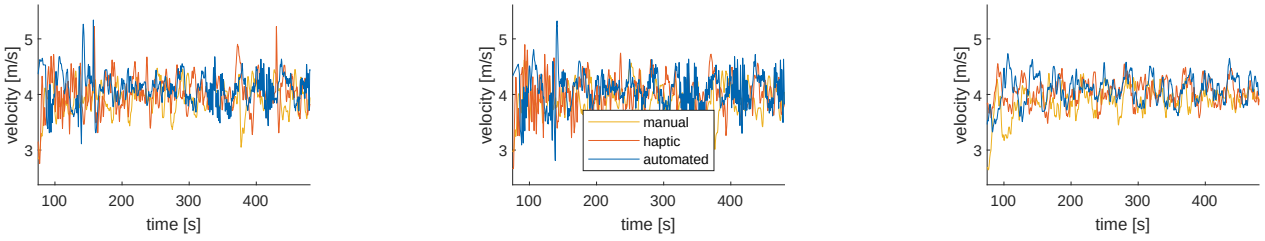

(a) following (b) ego (c) leading

Figure 55: plots of the velocity over time for each condition for the following vehicle, the ego vehicle and the leading vehicle

Participant 13

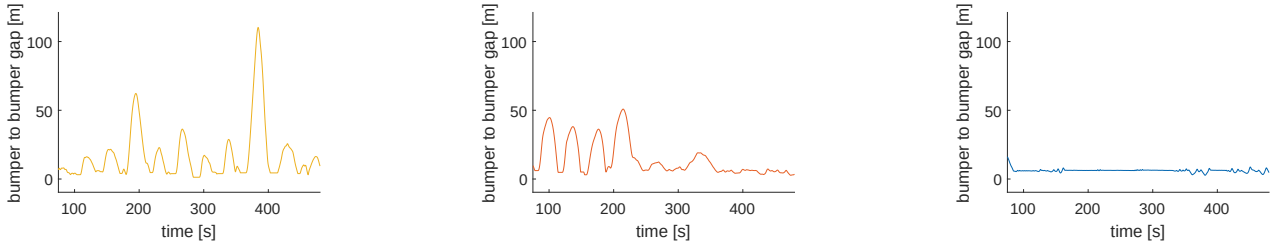

(a) manual (b) haptic (c) automatic

Figure 56: plots of the bumper to bumper gap between the ego vehicle and the leading vehicle over time for each condition

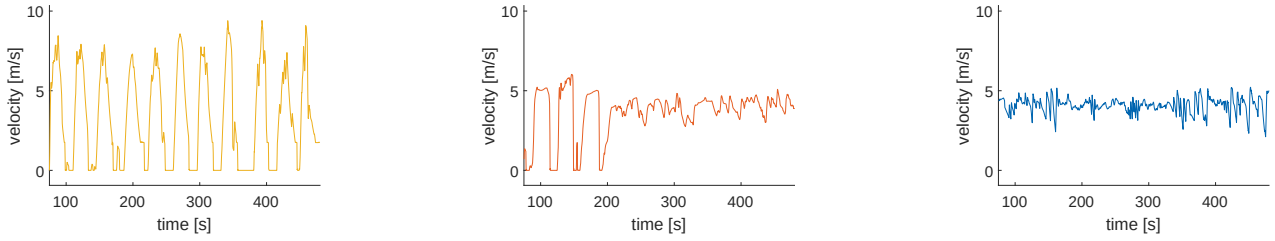

(a) manual (b) haptic (c) automated

Figure 57: plots of the velocity of the ego vehicle over time for each condition

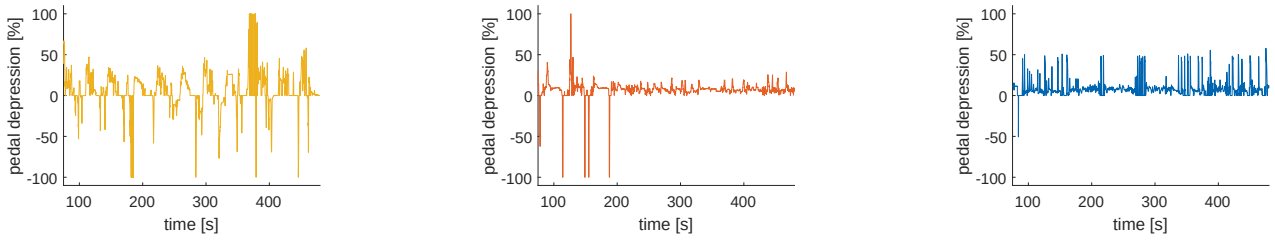

(a) manual (b) haptic (c) automated

Figure 58: plots of the pedal input of the ego vehicle over time for each condition. positive values correspond to accelerator pedal depression while negative values correspond to brake pedal depression

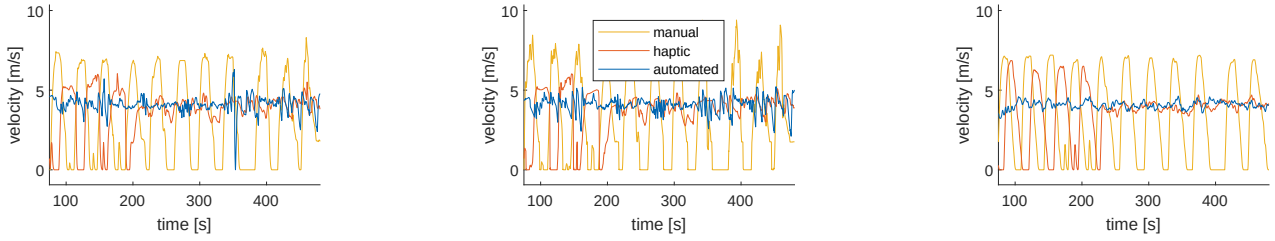

(a) following (b) ego (c) leading

Figure 59: plots of the velocity over time for each condition for the following vehicle, the ego vehicle and the leading vehicle

Participant 14

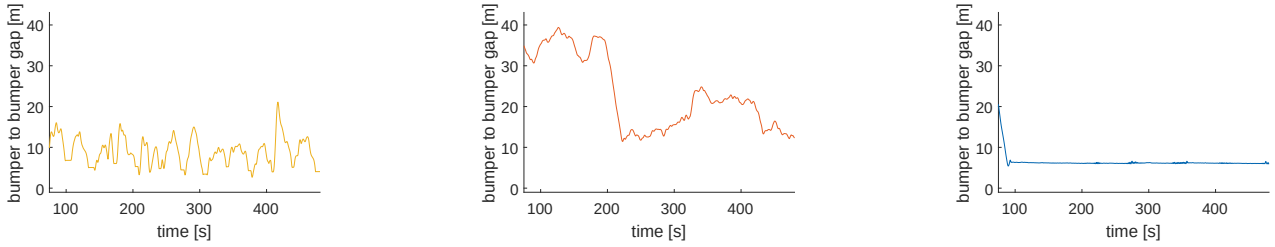

(a) manual (b) haptic (c) automatic

Figure 60: plots of the bumper to bumper gap between the ego vehicle and the leading vehicle over time for each condition

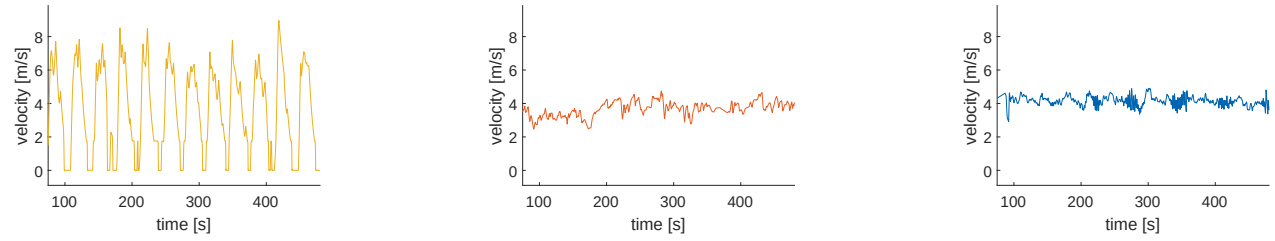

(a) manual (b) haptic (c) automated

Figure 61: plots of the velocity of the ego vehicle over time for each condition

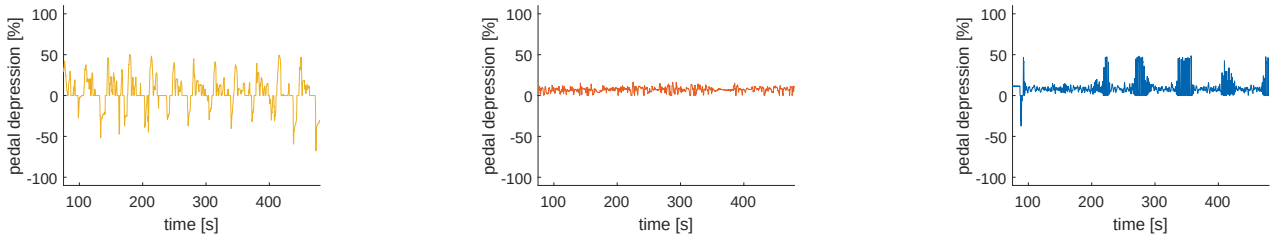

(a) manual (b) haptic (c) automated

Figure 62: plots of the pedal input of the ego vehicle over time for each condition. positive values correspond to accelerator pedal depression while negative values correspond to brake pedal depression

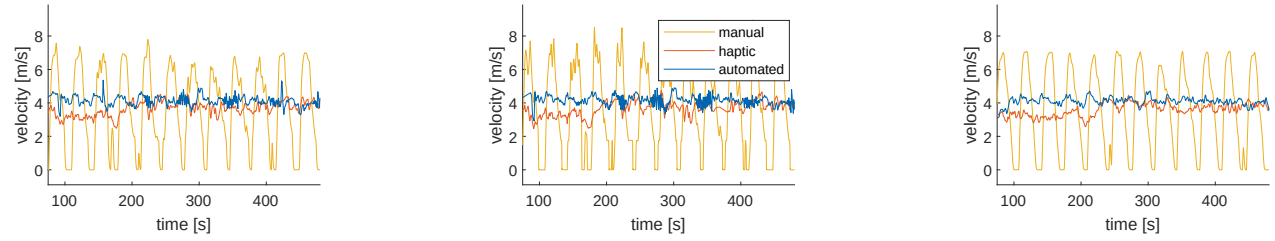

(a) following (b) ego (c) leading

Figure 63: plots of the velocity over time for each condition for the following vehicle, the ego vehicle and the leading vehicle

Participant 15

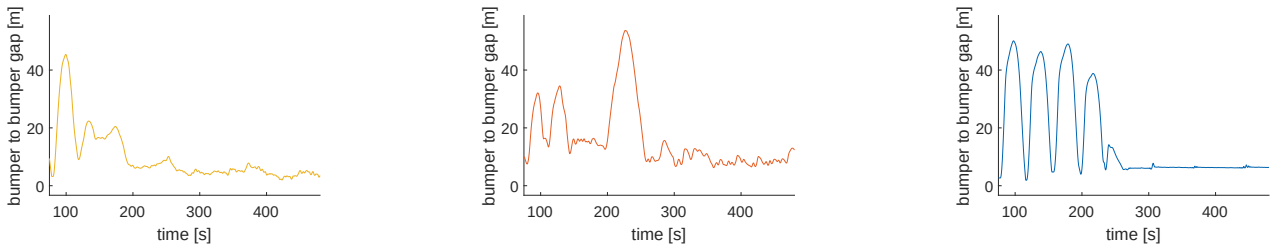

(a) manual (b) haptic (c) automatic

Figure 64: plots of the bumper to bumper gap between the ego vehicle and the leading vehicle over time for each condition

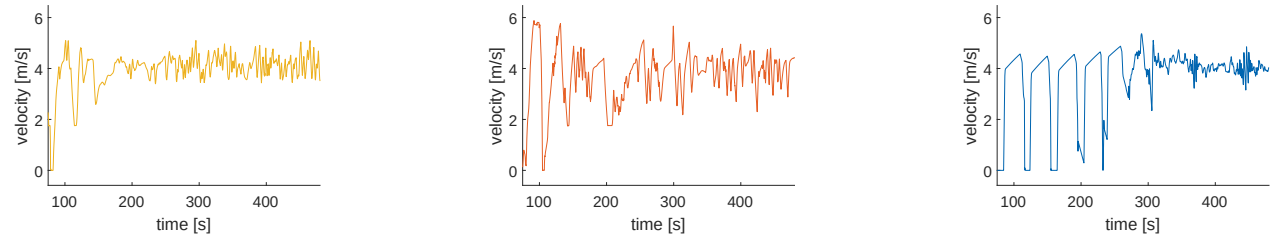

(a) manual (b) haptic (c) automated

Figure 65: plots of the velocity of the ego vehicle over time for each condition

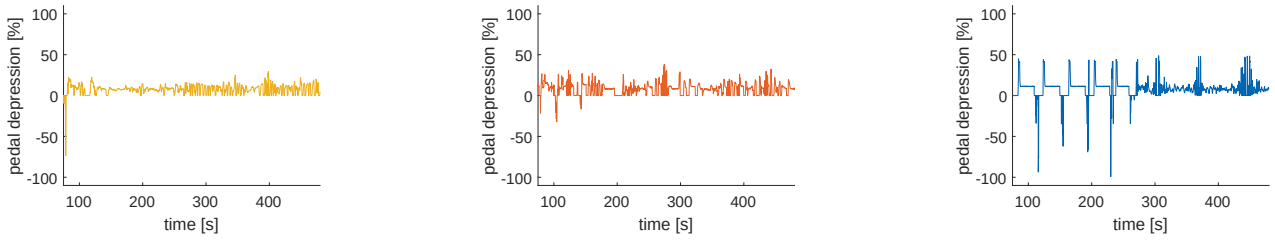

(a) manual (b) haptic (c) automated

Figure 66: plots of the pedal input of the ego vehicle over time for each condition. positive values correspond to accelerator pedal depression while negative values correspond to brake pedal depression

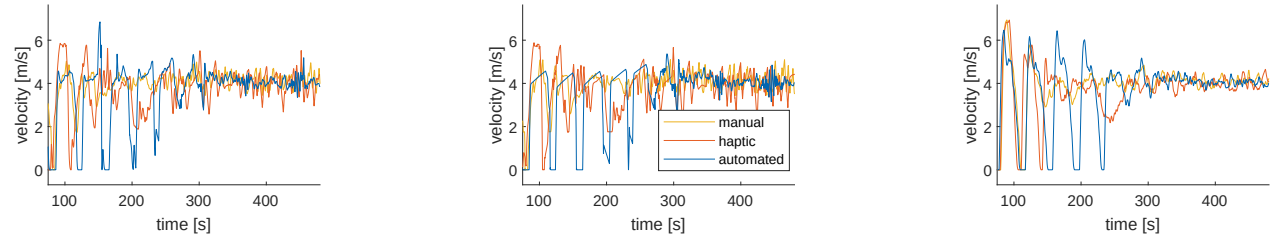

(a) following (b) ego (c) leading

Figure 67: plots of the velocity over time for each condition for the following vehicle, the ego vehicle and the leading vehicle

Participant 16

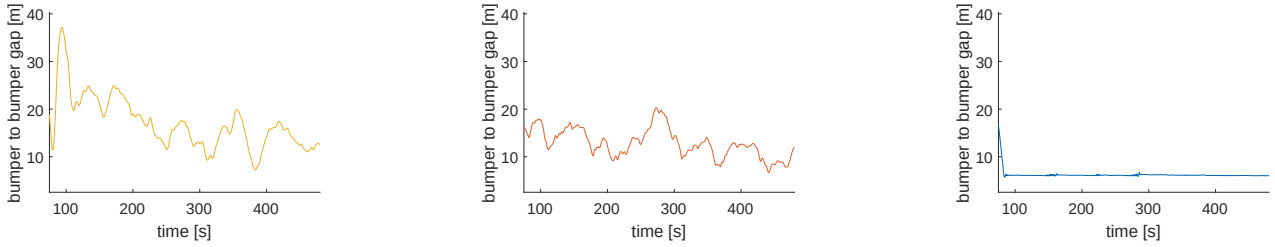

(a) manual (b) haptic (c) automatic

Figure 68: plots of the bumper to bumper gap between the ego vehicle and the leading vehicle over time for each condition

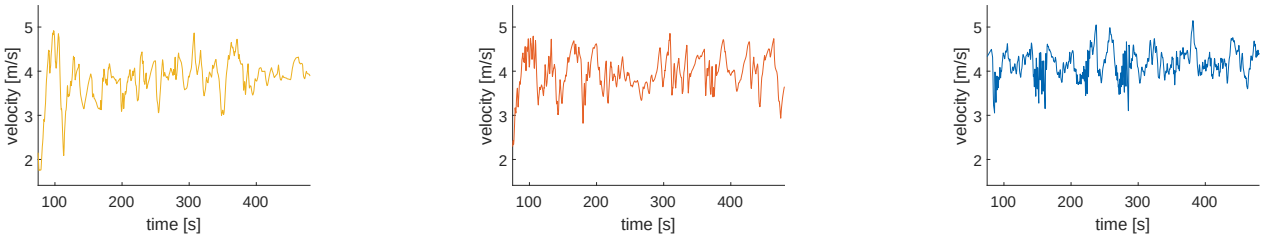

(a) manual (b) haptic (c) automated

Figure 69: plots of the velocity of the ego vehicle over time for each condition

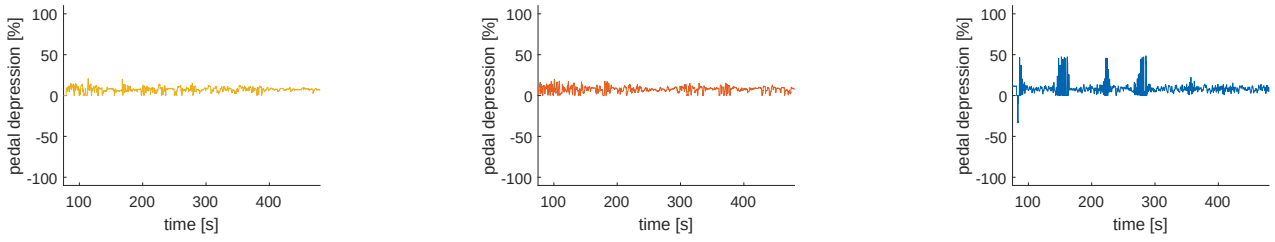

(a) manual (b) haptic (c) automated

Figure 70: plots of the pedal input of the ego vehicle over time for each condition. positive values correspond to accelerator pedal depression while negative values correspond to brake pedal depression

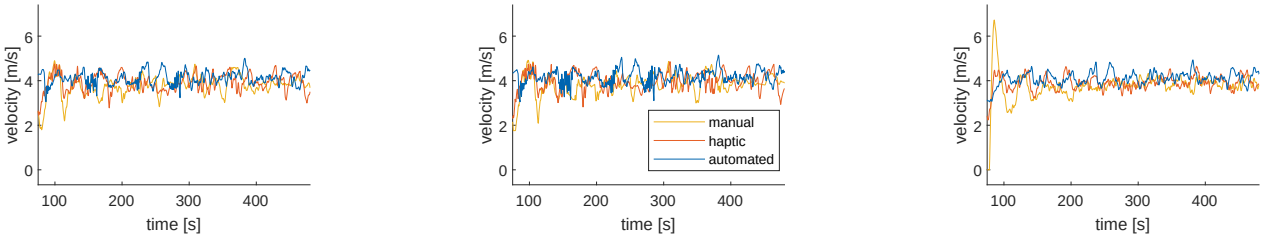

(a) following (b) ego (c) leading

Figure 71: plots of the velocity over time for each condition for the following vehicle, the ego vehicle and the leading vehicle

Participant 17

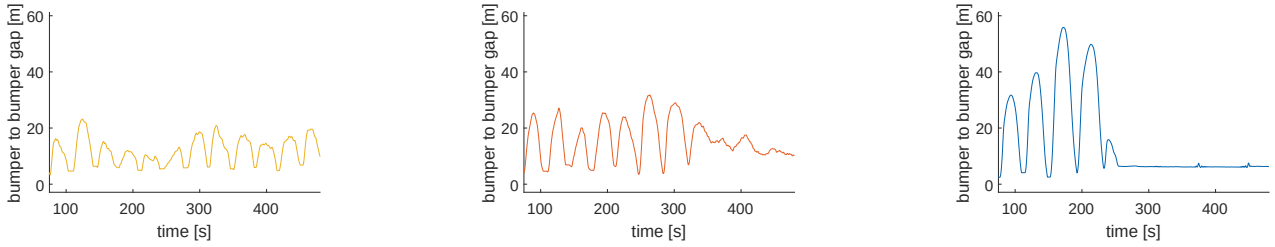

(a) manual (b) haptic (c) automatic

Figure 72: plots of the bumper to bumper gap between the ego vehicle and the leading vehicle over time for each condition

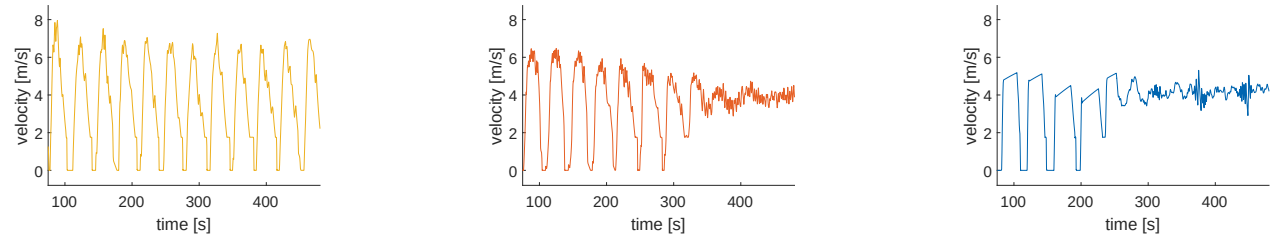

(a) manual (b) haptic (c) automated

Figure 73: plots of the velocity of the ego vehicle over time for each condition

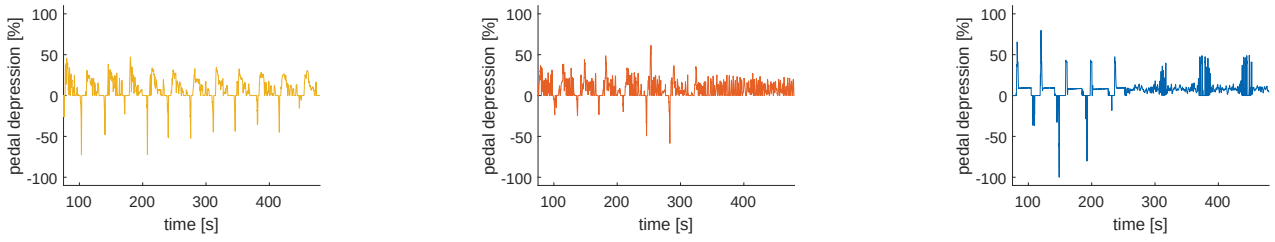

(a) manual (b) haptic (c) automated

Figure 74: plots of the pedal input of the ego vehicle over time for each condition. positive values correspond to accelerator pedal depression while negative values correspond to brake pedal depression

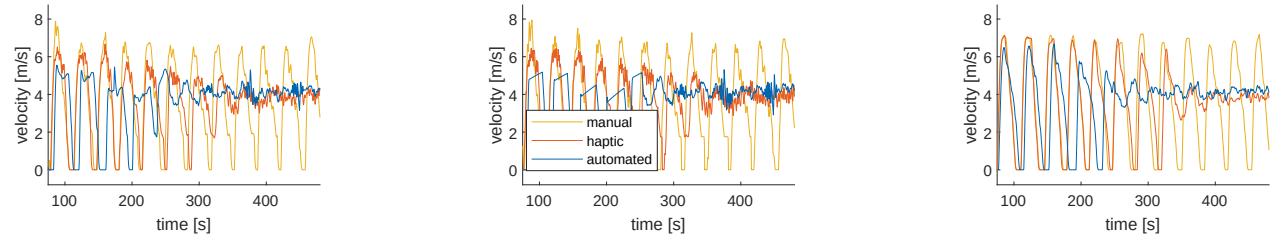

(a) following (b) ego (c) leading

Figure 75: plots of the velocity over time for each condition for the following vehicle, the ego vehicle and the leading vehicle

Participant 18

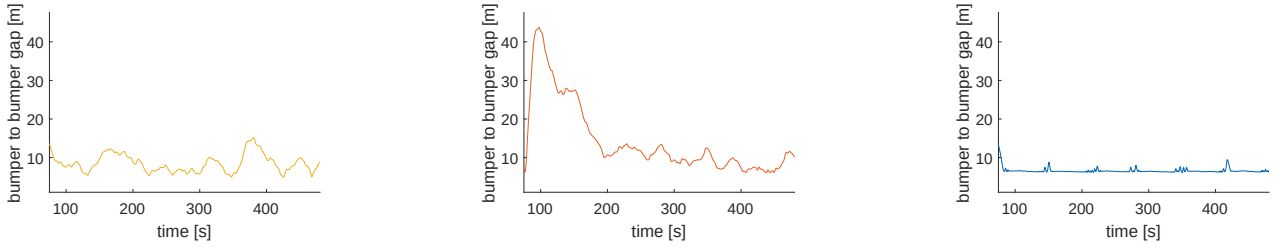

(a) manual (b) haptic (c) automatic

Figure 76: plots of the bumper to bumper gap between the ego vehicle and the leading vehicle over time for each condition

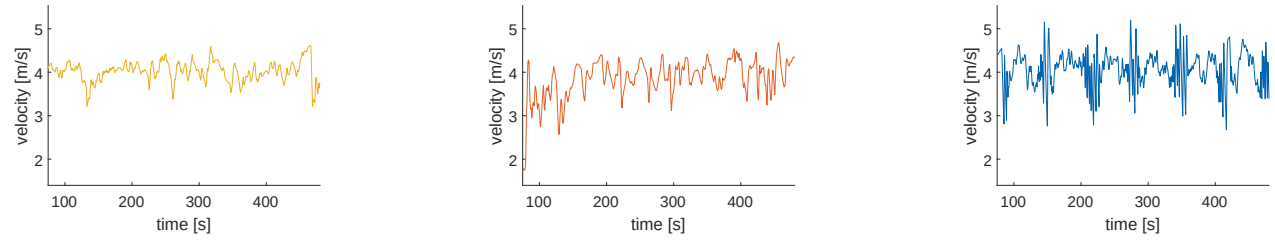

(a) manual (b) haptic (c) automated

Figure 77: plots of the velocity of the ego vehicle over time for each condition

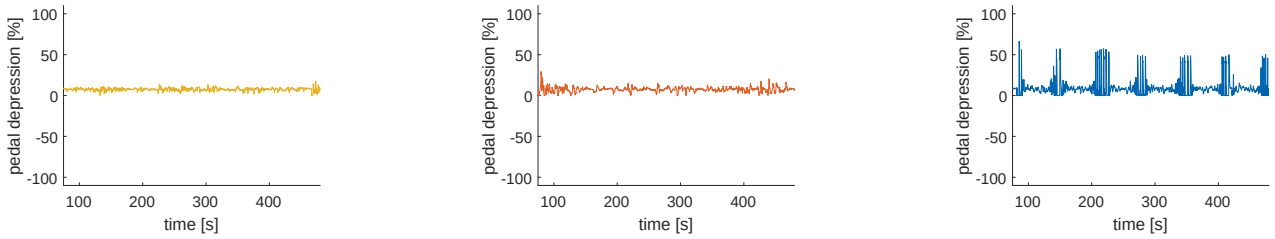

(a) manual (b) haptic (c) automated

Figure 78: plots of the pedal input of the ego vehicle over time for each condition. positive values correspond to accelerator pedal depression while negative values correspond to brake pedal depression

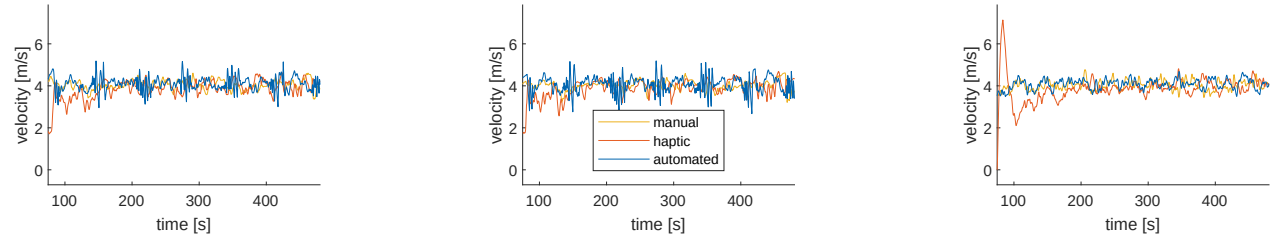

(a) following (b) ego (c) leading

Figure 79: plots of the velocity over time for each condition for the following vehicle, the ego vehicle and the leading vehicle

Participant 19

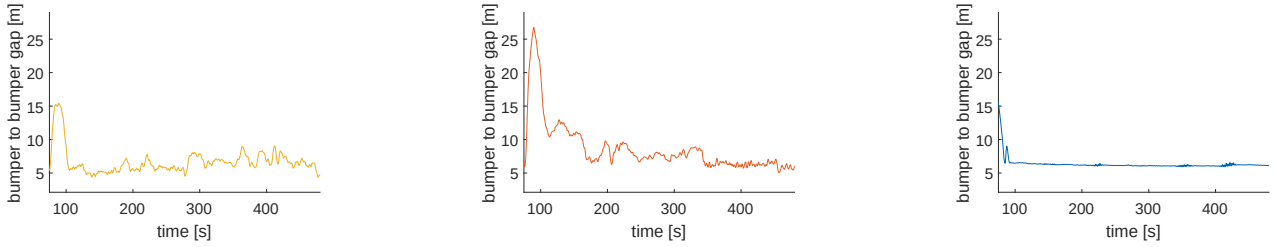

(a) manual (b) haptic (c) automatic

Figure 80: plots of the bumper to bumper gap between the ego vehicle and the leading vehicle over time for each condition

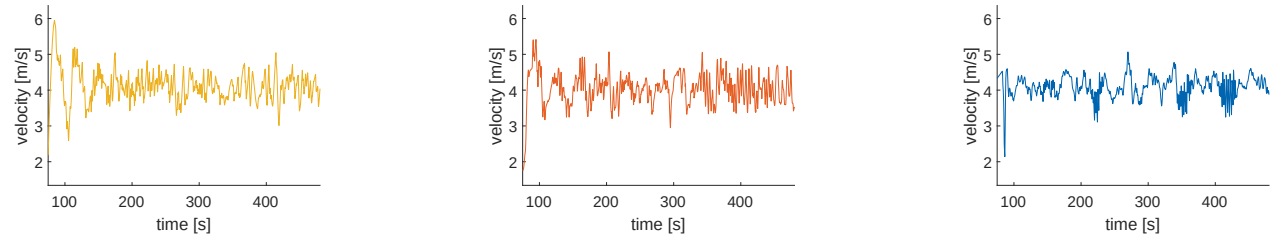

(a) manual (b) haptic (c) automated

Figure 81: plots of the velocity of the ego vehicle over time for each condition

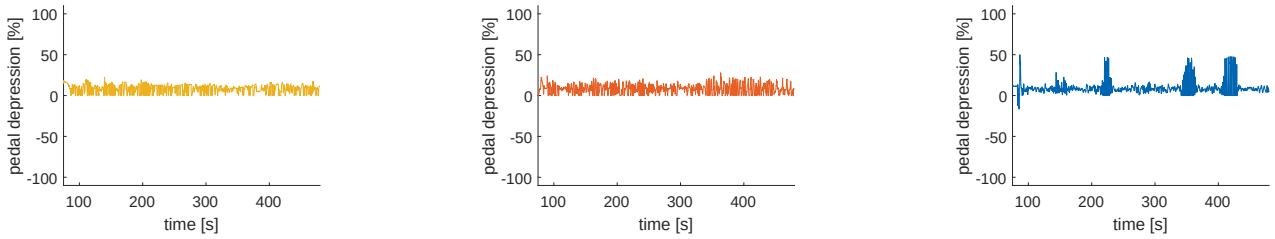

(a) manual (b) haptic (c) automated

Figure 82: plots of the pedal input of the ego vehicle over time for each condition. positive values correspond to accelerator pedal depression while negative values correspond to brake pedal depression

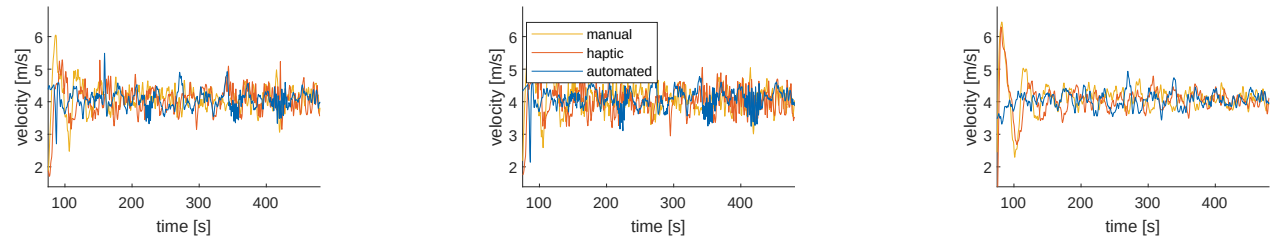

(a) following (b) ego (c) leading

Figure 83: plots of the velocity over time for each condition for the following vehicle, the ego vehicle and the leading vehicle

Participant 20

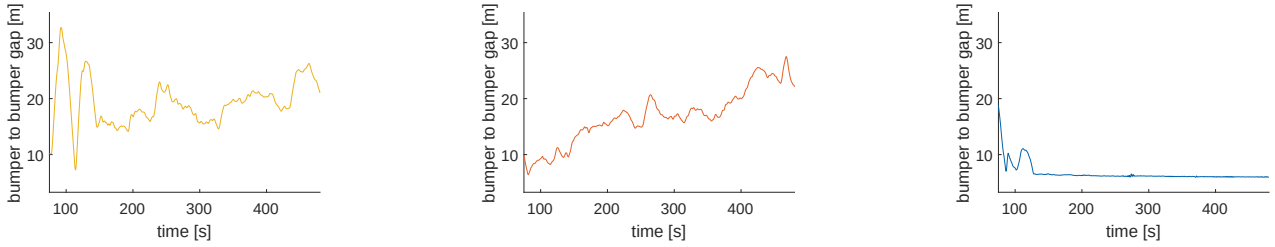

(a) manual (b) haptic (c) automatic

Figure 84: plots of the bumper to bumper gap between the ego vehicle and the leading vehicle over time for each condition

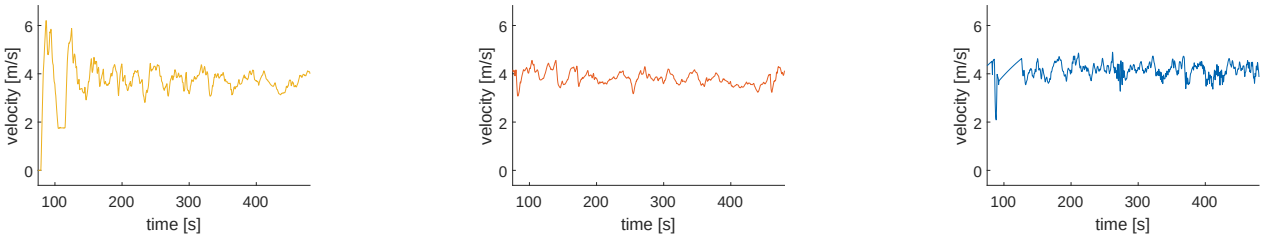

(a) manual (b) haptic (c) automated

Figure 85: plots of the velocity of the ego vehicle over time for each condition

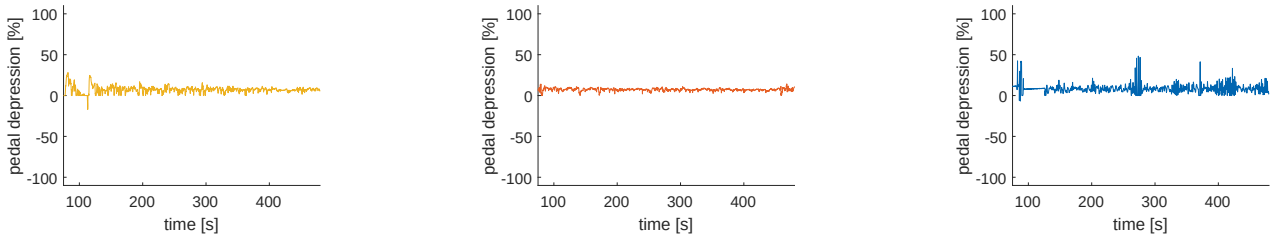

(a) manual (b) haptic (c) automated

Figure 86: plots of the pedal input of the ego vehicle over time for each condition. positive values correspond to accelerator pedal depression while negative values correspond to brake pedal depression

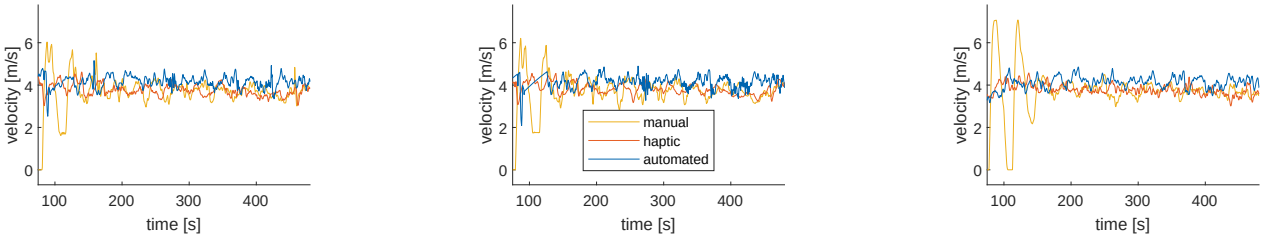

(a) following (b) ego (c) leading

Figure 87: plots of the velocity over time for each condition for the following vehicle, the ego vehicle and the leading vehicle

Participant 21

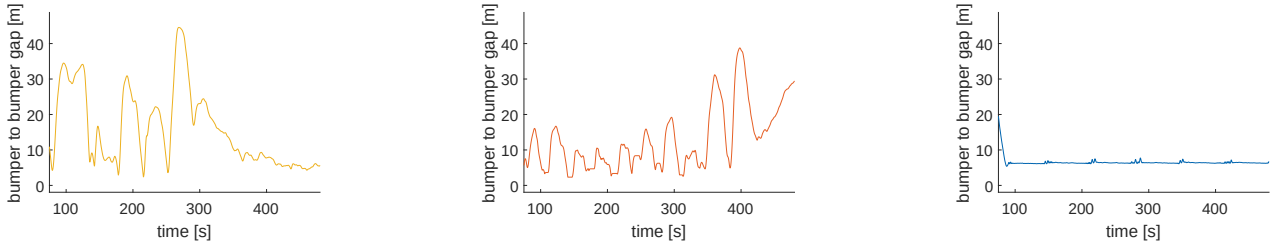

(a) manual (b) haptic (c) automatic

Figure 88: plots of the bumper to bumper gap between the ego vehicle and the leading vehicle over time for each condition

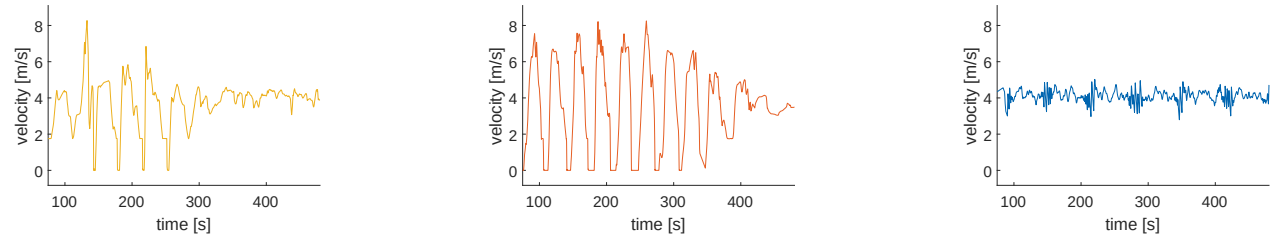

(a) manual (b) haptic (c) automated

Figure 89: plots of the velocity of the ego vehicle over time for each condition

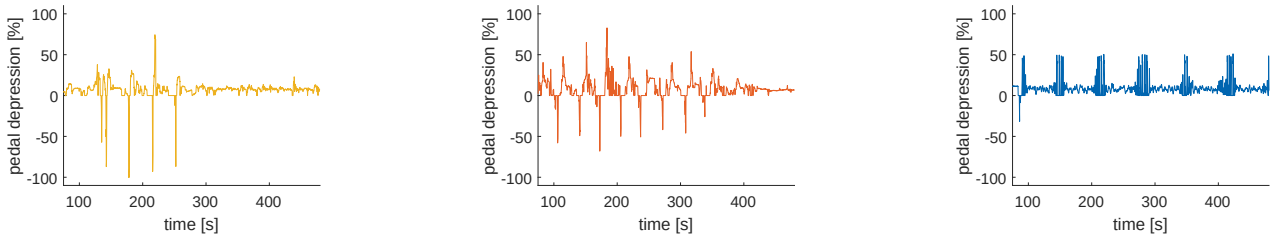

(a) manual (b) haptic (c) automated

Figure 90: plots of the pedal input of the ego vehicle over time for each condition. positive values correspond to accelerator pedal depression while negative values correspond to brake pedal depression

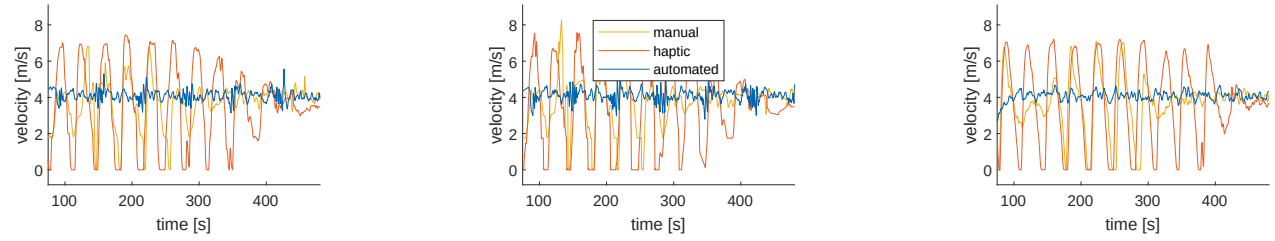

(a) following (b) ego (c) leading

Figure 91: plots of the velocity over time for each condition for the following vehicle, the ego vehicle and the leading vehicle

Participant 22

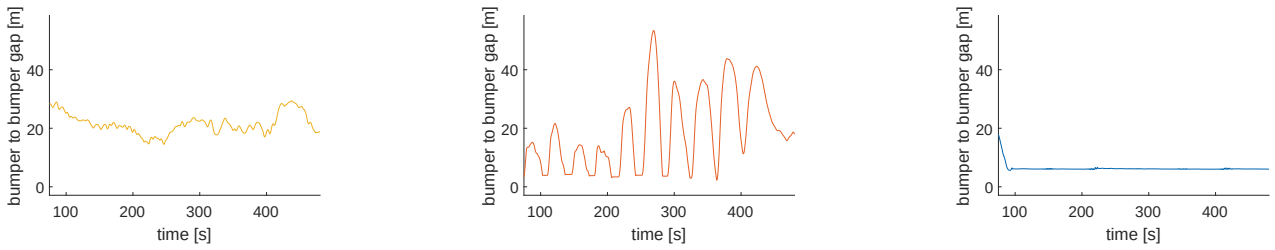

(a) manual (b) haptic (c) automatic

Figure 92: plots of the bumper to bumper gap between the ego vehicle and the leading vehicle over time for each condition

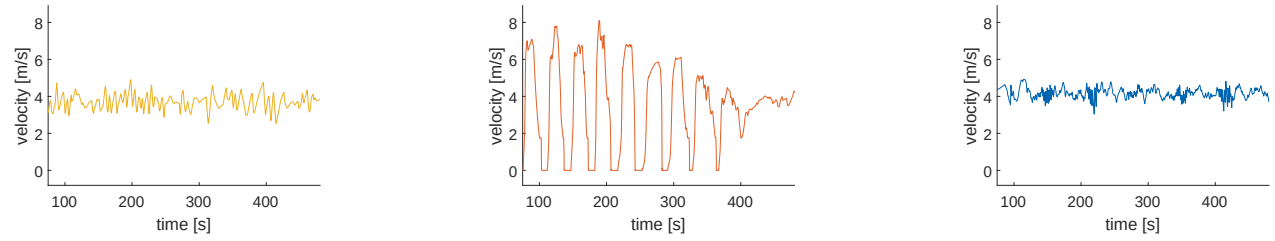

(a) manual (b) haptic (c) automated

Figure 93: plots of the velocity of the ego vehicle over time for each condition

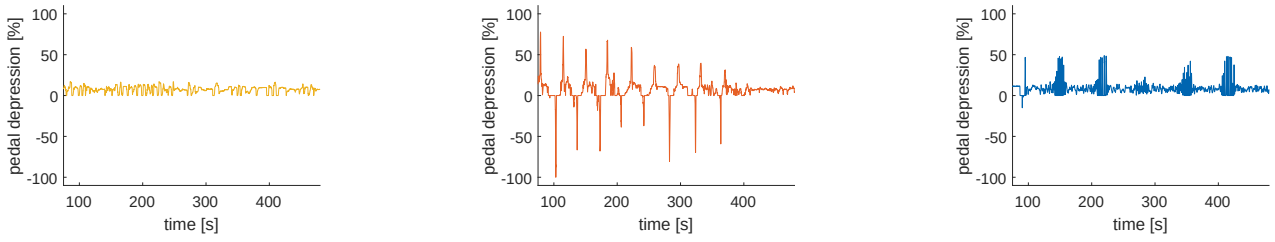

(a) manual (b) haptic (c) automated

Figure 94: plots of the pedal input of the ego vehicle over time for each condition. positive values correspond to accelerator pedal depression while negative values correspond to brake pedal depression

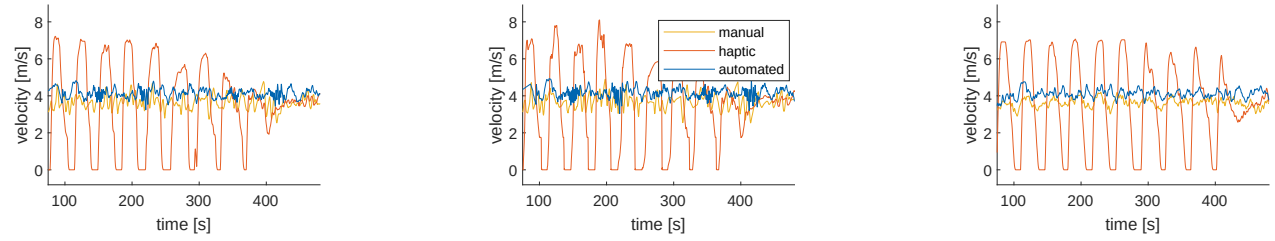

(a) following (b) ego (c) leading

Figure 95: plots of the velocity over time for each condition for the following vehicle, the ego vehicle and the leading vehicle

Participant 23

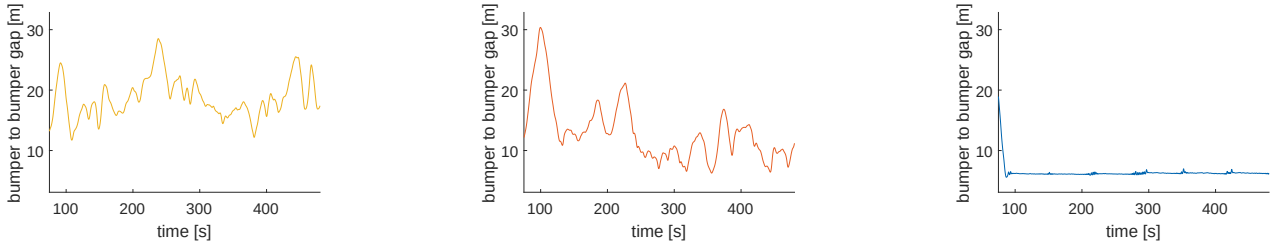

(a) manual (b) haptic (c) automatic

Figure 96: plots of the bumper to bumper gap between the ego vehicle and the leading vehicle over time for each condition

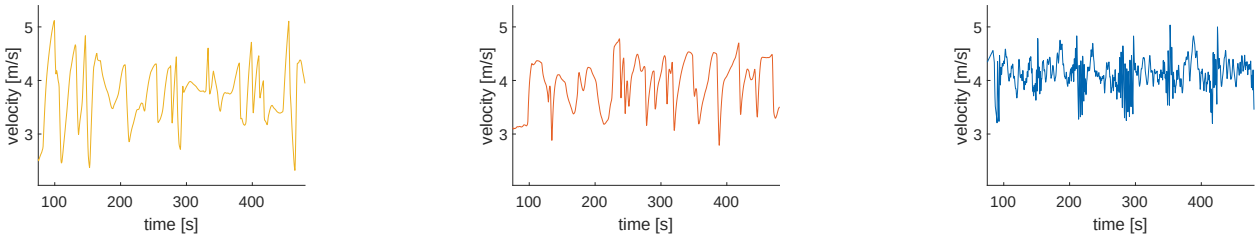

(a) manual (b) haptic (c) automated

Figure 97: plots of the velocity of the ego vehicle over time for each condition

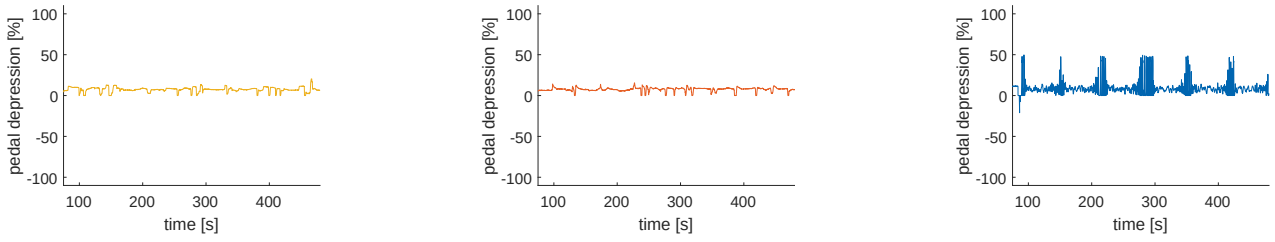

(a) manual (b) haptic (c) automated

Figure 98: plots of the pedal input of the ego vehicle over time for each condition. positive values correspond to accelerator pedal depression while negative values correspond to brake pedal depression

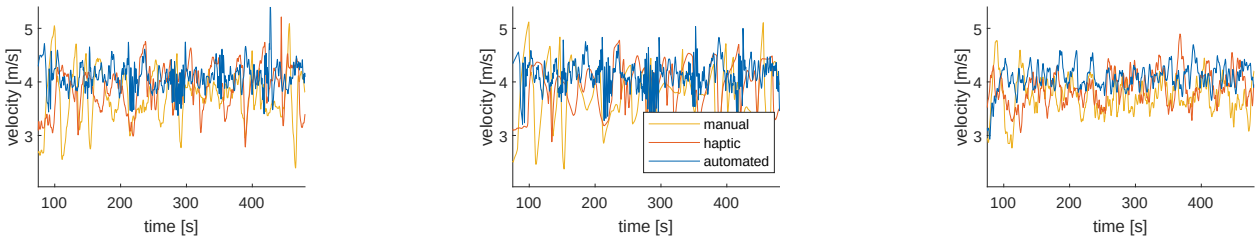

(a) following (b) ego (c) leading

Figure 99: plots of the velocity over time for each condition for the following vehicle, the ego vehicle and the leading vehicle

Participant 24

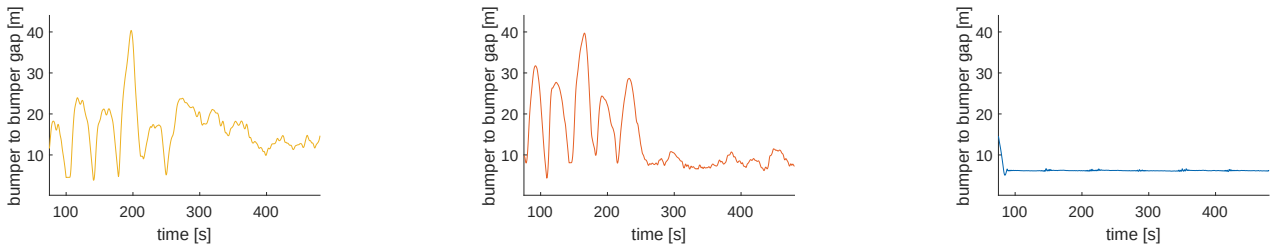

(a) manual (b) haptic (c) automatic

Figure 100: plots of the bumper to bumper gap between the ego vehicle and the leading vehicle over time for each condition

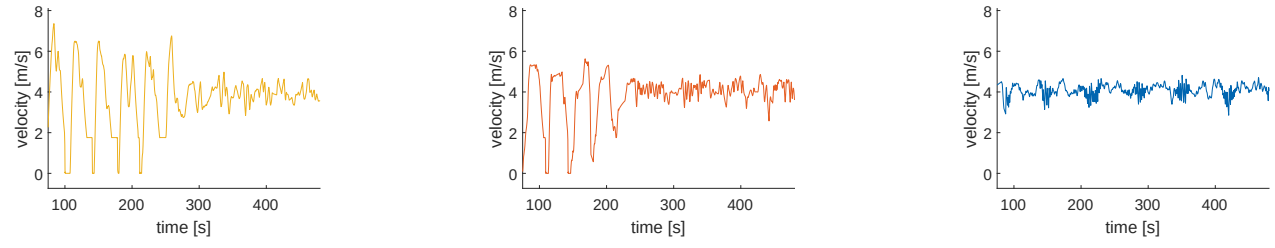

(a) manual (b) haptic (c) automated

Figure 101: plots of the velocity of the ego vehicle over time for each condition

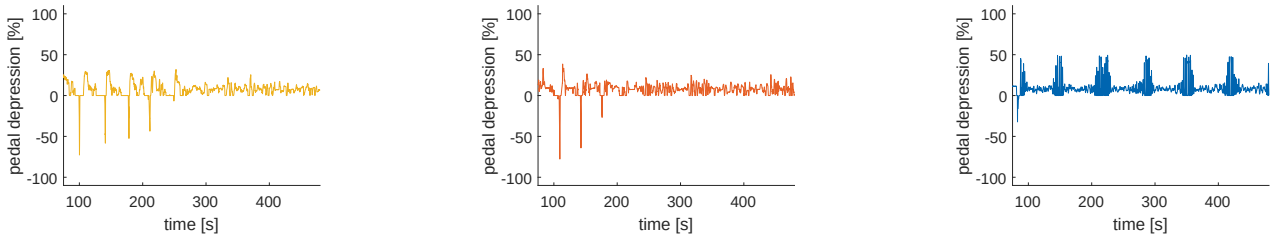

(a) manual (b) haptic (c) automated

Figure 102: plots of the pedal input of the ego vehicle over time for each condition. positive values correspond to accelerator pedal depression while negative values correspond to brake pedal depression

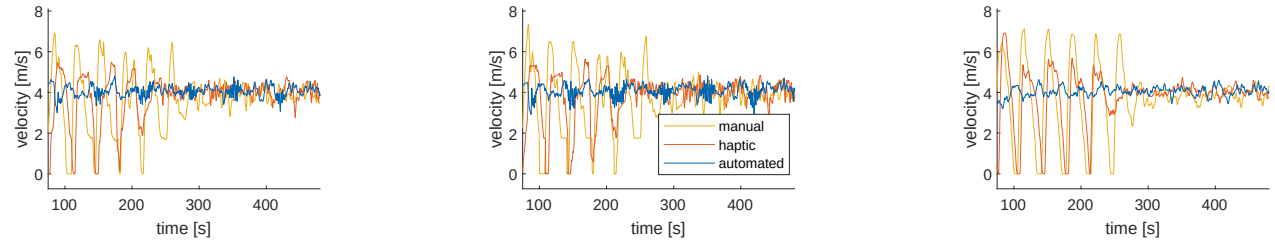

(a) following (b) ego (c) leading

Figure 103: plots of the velocity over time for each condition for the following vehicle, the ego vehicle and the leading vehicle

Participant 25

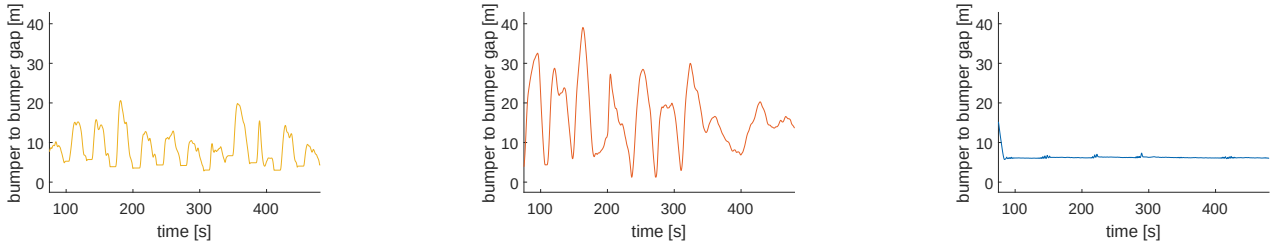

(a) manual (b) haptic (c) automatic

Figure 104: plots of the bumper to bumper gap between the ego vehicle and the leading vehicle over time for each condition

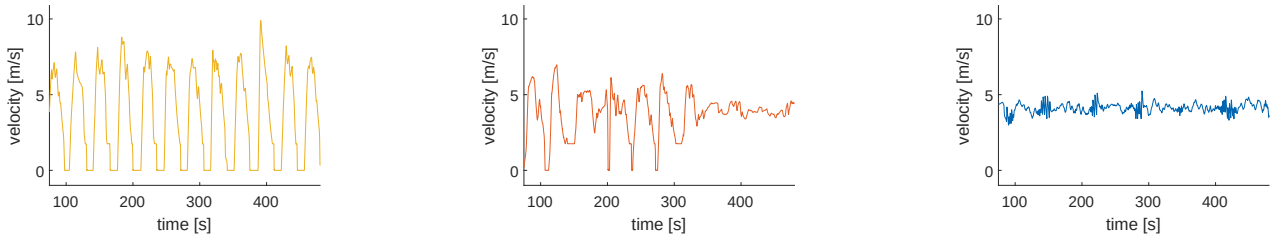

(a) manual (b) haptic (c) automated

Figure 105: plots of the velocity of the ego vehicle over time for each condition

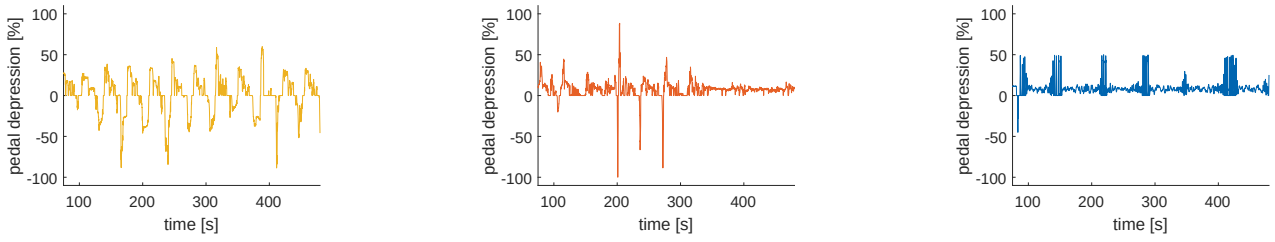

(a) manual (b) haptic (c) automated

Figure 106: plots of the pedal input of the ego vehicle over time for each condition. positive values correspond to accelerator pedal depression while negative values correspond to brake pedal depression

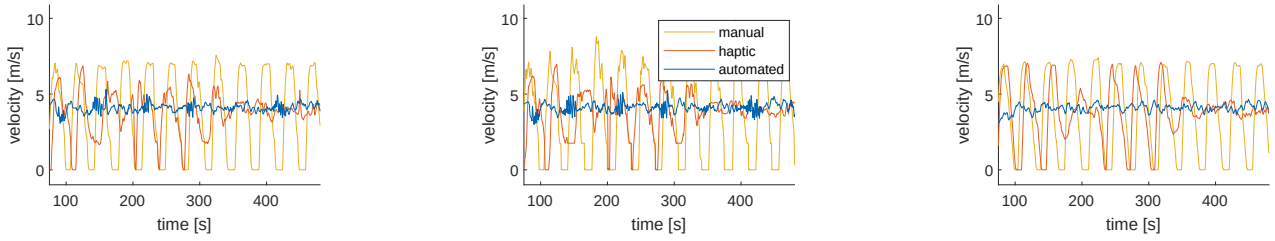

(a) following (b) ego (c) leading

Figure 107: plots of the velocity over time for each condition for the following vehicle, the ego vehicle and the leading vehicle

Participant 26

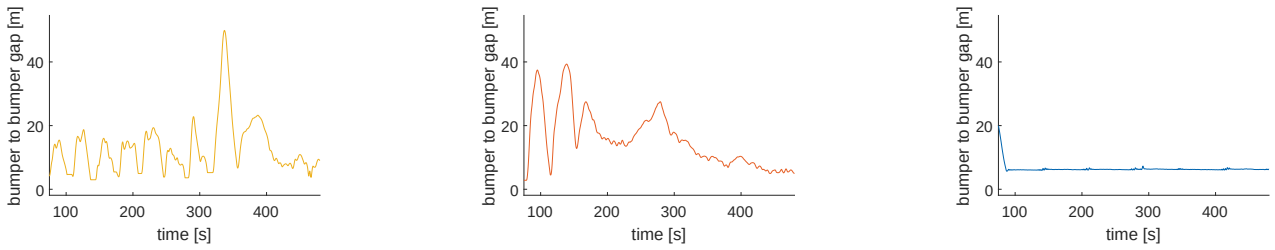

(a) manual (b) haptic (c) automatic

Figure 108: plots of the bumper to bumper gap between the ego vehicle and the leading vehicle over time for each condition

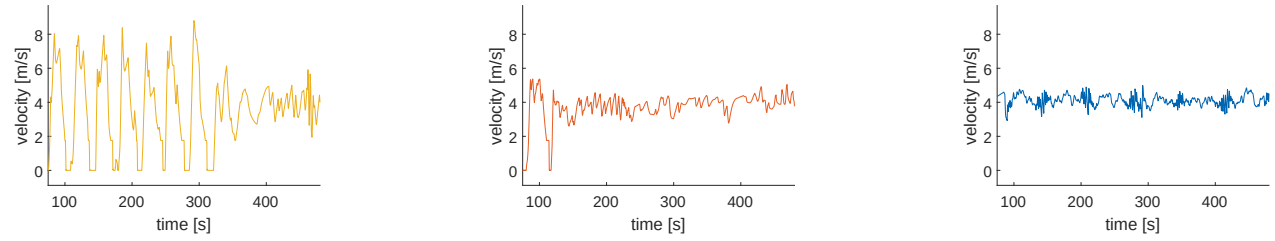

(a) manual (b) haptic (c) automated

Figure 109: plots of the velocity of the ego vehicle over time for each condition

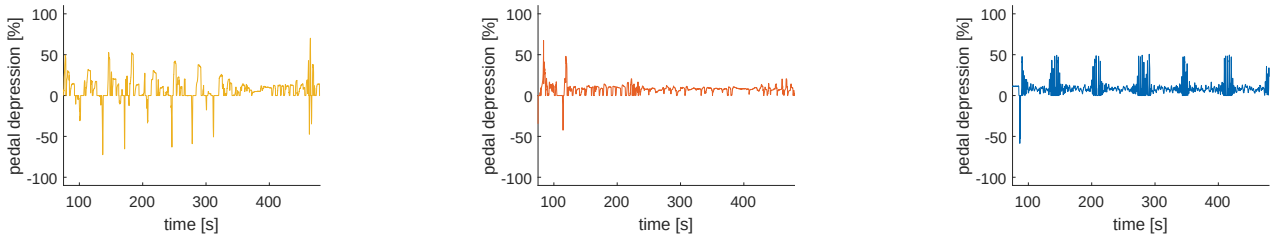

(a) manual (b) haptic (c) automated

Figure 110: plots of the pedal input of the ego vehicle over time for each condition. positive values correspond to accelerator pedal depression while negative values correspond to brake pedal depression

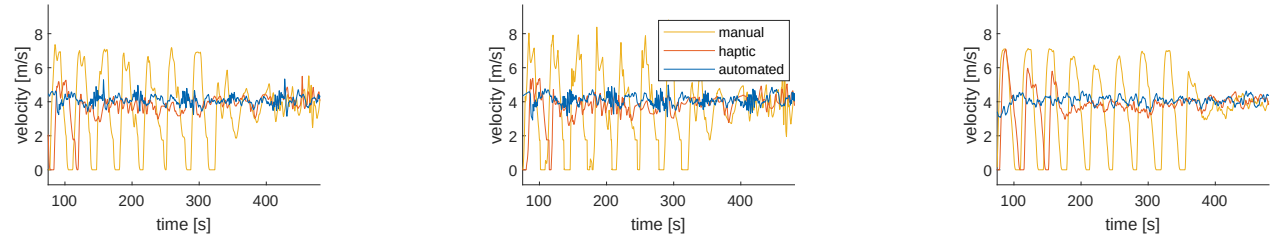

(a) following (b) ego (c) leading

Figure 111: plots of the velocity over time for each condition for the following vehicle, the ego vehicle and the leading vehicle

Participant 27

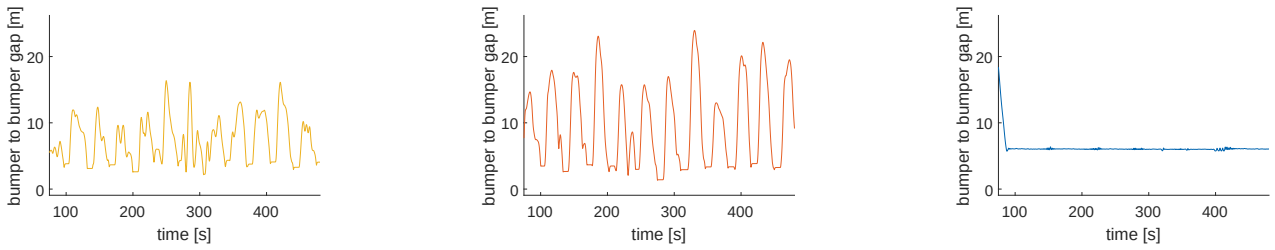

(a) manual (b) haptic (c) automatic

Figure 112: plots of the bumper to bumper gap between the ego vehicle and the leading vehicle over time for each condition

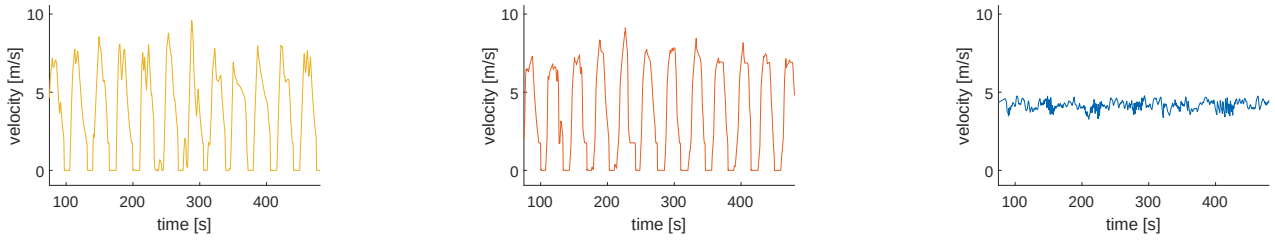

(a) manual (b) haptic (c) automated

Figure 113: plots of the velocity of the ego vehicle over time for each condition

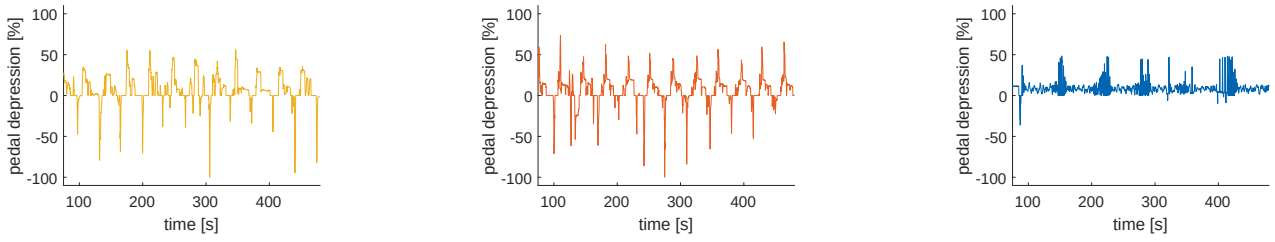

(a) manual (b) haptic (c) automated

Figure 114: plots of the pedal input of the ego vehicle over time for each condition. positive values correspond to accelerator pedal depression while negative values correspond to brake pedal depression

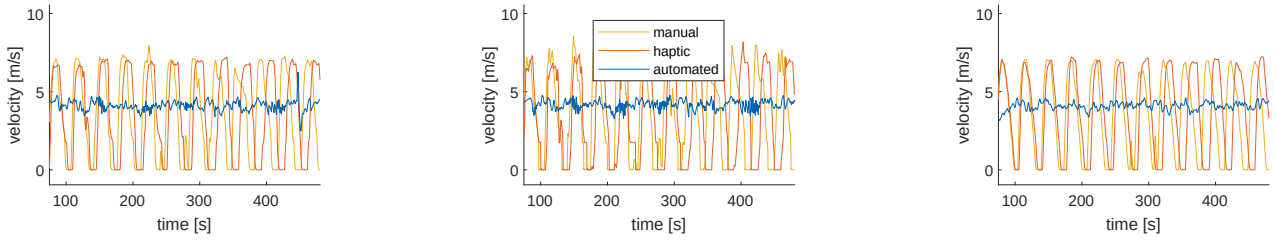

(a) following (b) ego (c) leading

Figure 115: plots of the velocity over time for each condition for the following vehicle, the ego vehicle and the leading vehicle

Participant 28

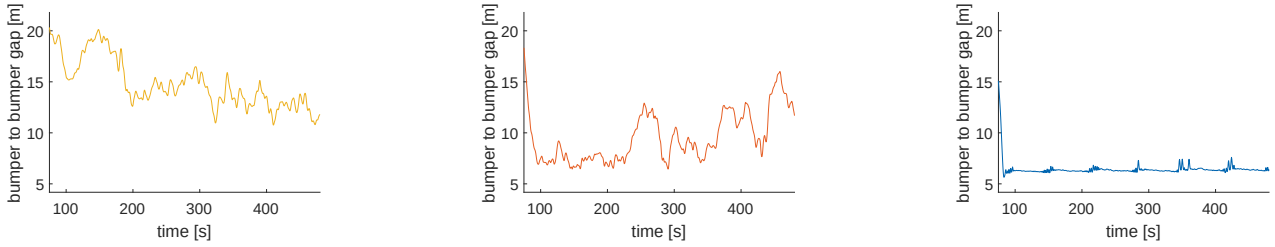

(a) manual (b) haptic (c) automatic

Figure 116: plots of the bumper to bumper gap between the ego vehicle and the leading vehicle over time for each condition

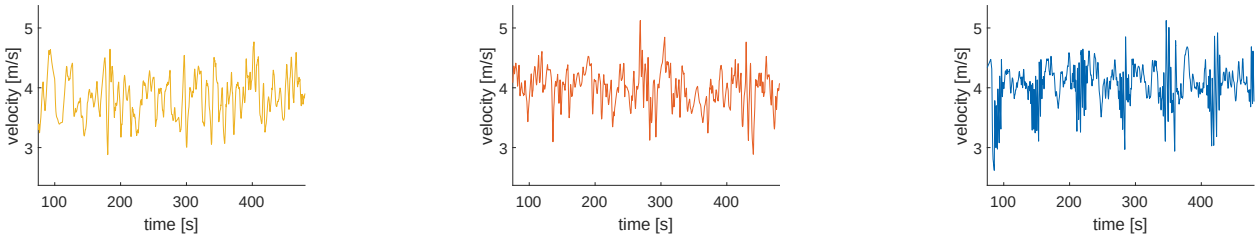

(a) manual (b) haptic (c) automated

Figure 117: plots of the velocity of the ego vehicle over time for each condition

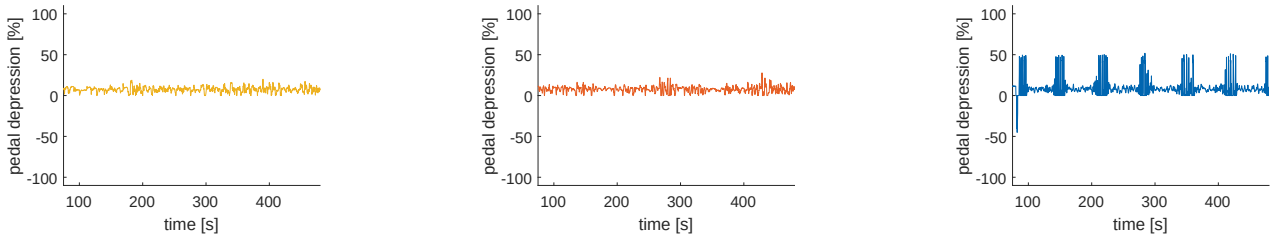

(a) manual (b) haptic (c) automated

Figure 118: plots of the pedal input of the ego vehicle over time for each condition. positive values correspond to accelerator pedal depression while negative values correspond to brake pedal depression

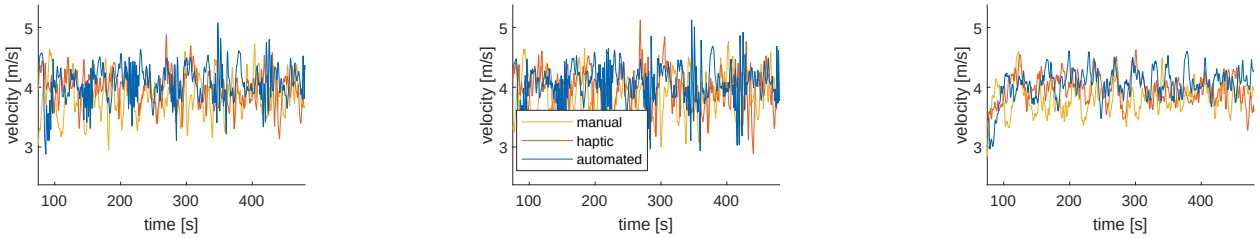

(a) following (b) ego (c) leading

Figure 119: plots of the velocity over time for each condition for the following vehicle, the ego vehicle and the leading vehicle

Participant 29

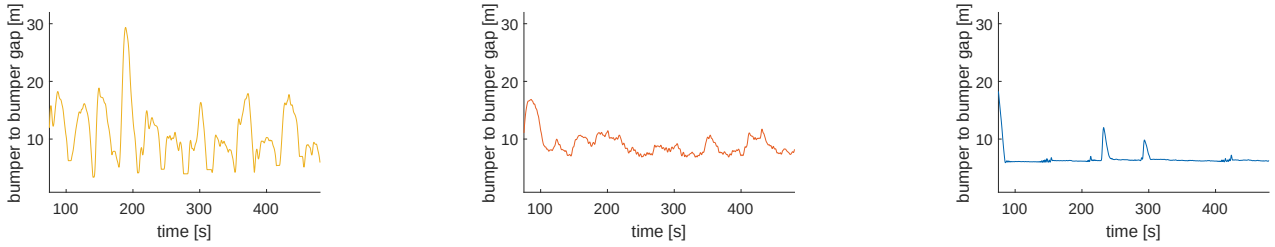

(a) manual (b) haptic (c) automatic

Figure 120: plots of the bumper to bumper gap between the ego vehicle and the leading vehicle over time for each condition

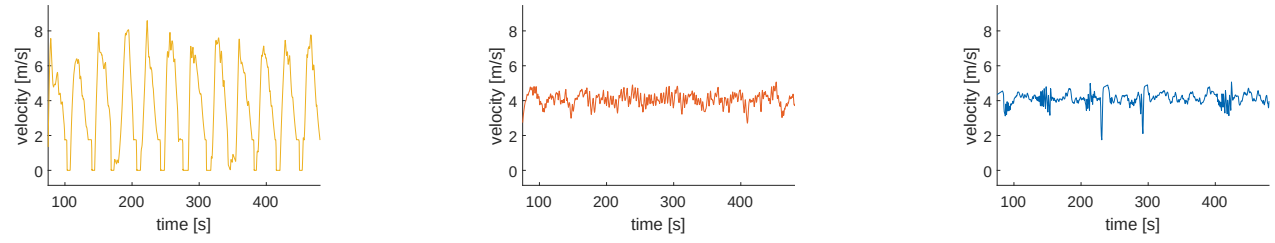

(a) manual (b) haptic (c) automated

Figure 121: plots of the velocity of the ego vehicle over time for each condition

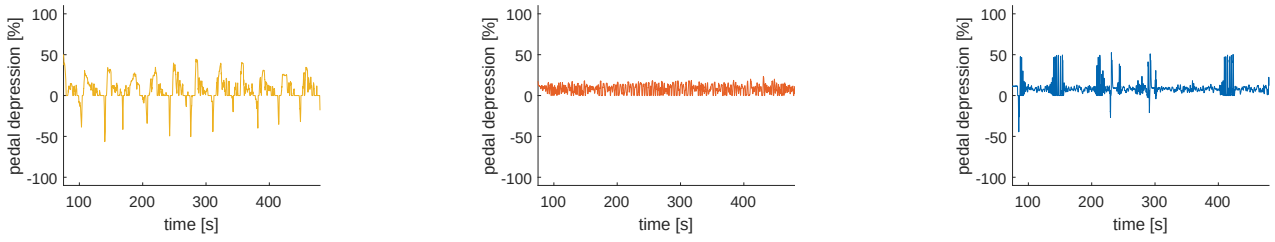

(a) manual (b) haptic (c) automated

Figure 122: plots of the pedal input of the ego vehicle over time for each condition. positive values correspond to accelerator pedal depression while negative values correspond to brake pedal depression

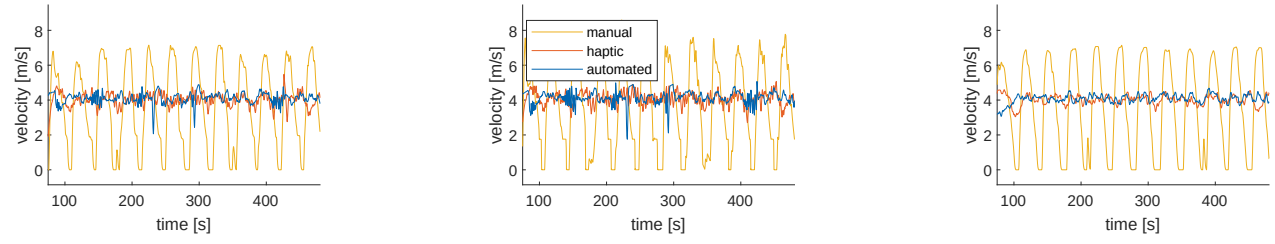

(a) following (b) ego (c) leading

Figure 123: plots of the velocity over time for each condition for the following vehicle, the ego vehicle and the leading vehicle

Appendix E: Forms

Informed Consent Form

1 Research Group

1.1 Researchers in charge of the project

Klaas Koerten[1]	Master Student	Delft University of Technology
Christiaan Koppel[2]	Project Engineer	Cruden B.V.
Arkady Zgonnikov[1]	Assistant Professor	Delft University of Technology
David Abbink[1]	Full Professor	Delft University of Technology

1.2 Organizations

1. Department of Cognitive Robotics; Faculty of Mechanical, Maritime and Materials Engineering; Delft University of Technology; Delft, the Netherlands
2. Cruden B.V.; Amsterdam, the Netherlands

---

2 This document

This informed consent form has two parts:

- **Information sheet,** pages 1-6
- **Consent form,** page 7

Before agreeing to participate in this study, you are asked to read this document carefully. The information sheet describes the purpose, procedures, and risks of this study. After reading the information sheet, feel free to ask questions about any part that seems unclear or sections that you do not understand. You should feel comfortable to speak to all of the researchers involved to answer any questions you may have at any time. After you have read this information sheet and all your question are answered and any concerns are discussed, you can decide if you would like to be involved. At the end of this document, we would like to ask you to sign a written consent form to confirm your agreement to participate. Your signature is required for participation.

---

3 Purpose of the research

A phantom traffic jams is a phenomenon that may occur on busy highways. Due to typical human driving behaviour, small disturbances in the traffic flow stability get amplified and generate typical stop-and-go waves. Because phantom traffic jams cause a reduction in the traffic throughput alongside increased fuel consumption and stress with the drivers, research is being done on how to prevent these traffic jams or dissolve them once they occur. The solution of these studies use full automation on the longitudinal vehicle motion. Although these studies look promising and have proven to be able to dissipate phantom traffic jams with a realistic amount of automated vehicles, they often do not take some of the downsides of automation into account. One of these downsides is the fact that automation could fail, which might result in

collisions, especially in a dense traffic situation. This experiment will evaluate an alternative system in which the driver controls the longitudinal motion of a car with an accelerator and brake pedal, but is assisted in this by guidance forces from a controller. This means of control is called haptic shared control and this study will evaluate the effectiveness of haptic shared control in dissipating and preventing phantom traffic jams. Furthermore, an evaluation will be done to determine the driver's acceptance of the controller.

---

4 Participation

4.1 Location of the experiment

Participation will involve completing a driving experiment on a driving simulator at Cruden B.V. Global Headquarters, Pedro de Medinalaan 25, 1086 XP Amsterdam, the Netherlands.

4.2 Eligibility criteria

You are invited to participate in this project if:

- You are 18 years or older.
- You have a car driving license.
- You have normal or corrected-to-normal vision (i.e. glasses or contact lenses).
- You have not experienced severe (simulator) motion sickness in the past.
- You do not have heart, back or neck issues.
- You have not been diagnosed with epilepsy.
- You are not pregnant.
- You have not recently had surgery.
- You are not physically disabled.
- You are not under the influence of drugs, alcohol or prescription substances that may compromise the comfort when operating a driving simulator.

The researchers reserve the right at any time to refuse or excuse any participant who no longer meets the study requirements or who are behaving in an unnecessarily unsafe manner.

4.3 Voluntary participation

Your participation in this project is completely voluntary. We welcome you to contact us to ask any questions and to discuss your possible involvement in the project, you have the right to refuse participation at any moment. If you do agree to participate you have the right to withdraw from the project at any moment without comment or penalty.

5 Procedure

The research consists of a driving experiment on a driving simulator. The experiment will save data about the traffic stability to evaluate the effectiveness of the proposed controller. The driving data will be logged by the driving simulator.

5.1 Prior to the experiment

Prior to the experiment, the informed consent form will be given to you. When you visit the location of the experiment, the study details will be explained to you and you will be asked to sign the informed consent form. After this, a demographics questionnaire will be completed for the statistical analysis of the results. Finally, a safety instruction for operating the driving simulator will be given.

5.2 Practice session on simulator

The experiment will start with some practice to familiarise yourself with the simulator, the virtual environment and the procedure of starting an experiment. The practice session takes around 5 minutes and you are encouraged to drive both fast and slow to get a feeling of the dynamics of the simulated car, the behaviour of the other traffic cars and the road.

5.3 Experiment

You will be asked to perform three driving sessions of approximately ten minutes in a driving scenario on a ring road. Between the sessions, there will be a short break. During driving, interaction with surrounding traffic will be simulated. The simulated vehicle is a generic car and is controlled in the same way as a normal automatic car. A dashboard with speedometer is available as well as a side view mirror.

5.3.1 Controls

The simulator contains the same controls for driving as a regular car. A steering wheel, accelerator and brake pedal are present to control the heading, acceleration and deceleration respectively. You are asked to keep a constant speed during the experiment using the gas and brake pedal. Please drive in a safe manner like you normally would and use the steering wheel for keeping the car in the single lane it starts in.

5.3.2 Scenario

Each driving session will take place on a closed ring road with a circumference of 260 meters. 21 cars, including the simulated car you are in, are evenly spaced out along this road. You will be asked to accelerate to a constant speed to follow the car ahead of you. The other cars will also start driving. You are asked to treat the other traffic cars as you would treat normal road users. For the duration of each session, you are asked to drive at a constant speed while not colliding with the traffic cars.

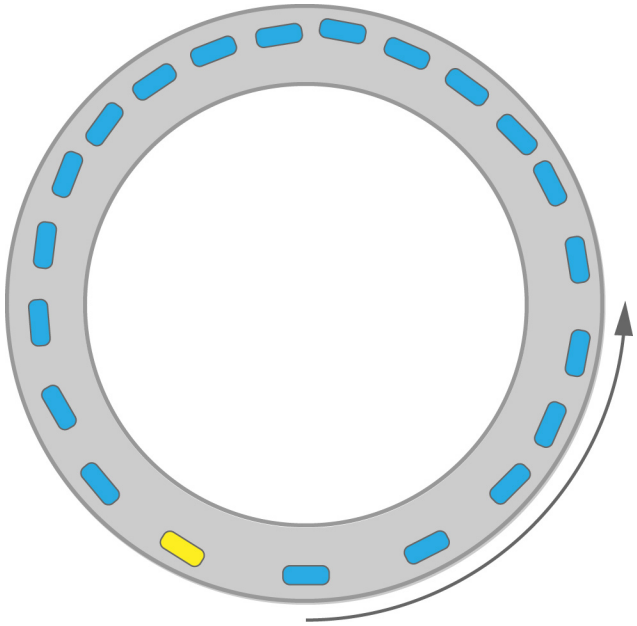

5.4 Duration

The total time commitment will amount to approximately 45 minutes and consists of reading and signing the consent form, driving in the simulator practice session, executing the three experiment sessions including breaks and completing the questionnaires.

5.5 COVID-19 precautions

To minimize the risk of COVID-19 infection for the participant and operator of the experiment, both are required to wear a face mask before and after the experiment. During the experiment, a safe distance of at least 2 meters is guaranteed. To minimize the risk of contagion amongst participants, all materials used during the experiment will be disinfected after each participant and a time buffer will be planned between participants to ensure their attendances will not overlap. The participant and the operator will be the only two people present on the location of the experiment.

---

6 Expected benefits

It is not expected that the project directly benefits you. However, your participation in this study will add to our understanding of Advanced Driver Assistance Systems (ADAS) and haptic shared control and the interaction of these systems with human drivers. In this way your participation will assist in developing new approaches to improve driver safety and comfort.

---

7 Risks associated with participation

In case a participant experiences any inconvenience or unpleasantness, the experiment can be stopped at any time. An emergency switch is available to the participant, which will stop the simulation immediately.

The simulator contains active pedals on which forces get applied during a simulation. During a simulation these pedals can move. It is therefore important that the participant only steps in or out of the seat of the simulator when the pedals are shut down. During the experiment, an operator ensures safe operation of the driving simulator. If the operator notices unsafe or unwanted behavior of the simulator or the participant, the experiment may be terminated prematurely.

Losing control of the vehicle can result in a collision with other cars. However, the surrounding vehicles are non-solid objects, so a participant can drive through them without physically experiencing a collision. Riding through a non-solid object can be an emotionally uncomfortable experience.

---

8 Privacy and confidentiality

All comments and responses are anonymous and will be treated confidentially. The names of individual persons are not required in any of the responses. Publications or presentations of the results will not include any information that could identify you.

Any data collected as part of this project will be stored securely as per TU Delft's Research Data Management Policy. Only the researchers involved in the project will have access to this information. Please note that non-identifiable data from this project may be used as comparative data in future projects or stored on an open access database for secondary analysis.

---

9 Responsibility

The researchers, funding bodies or institutions involved do not bear any responsibility for possible inconveniences or damages during travel to or from the location of the experimental activity.

---

10 Questions about the project

If you wish to ask questions about the project or require further information, please contact one of the researchers below:

Researcher	**E-mail**	**Phone**
Klaas Koerten	K.o.koerten@student.tudelft.nl	+31(0)6 27908800
Christiaan Koppel	C.Koppel@cruden.com	
Arkady Zgonnikov	A.zgonnikov@tudelft.nl	
David Abbink	D.A.Abbink@tudelft.nl	

---

11 Ethical approval and complaints

This study has been approved by the Human Research Ethics Committee (HREC). If needed, verification of approval can be obtained by writing to the mail or e-mail address of the HREC, noted at the end of this section. If you have any concerns or complaints about the ethical conduct of the project, any of the aforementioned involved researchers can be contacted. In case this does not resolve your concern you may contact the HREC, which is not connected with the research project and can facilitate a solution to your concern in an impartial manner. Name of the experiment according to the Ethics Approval Application: *Longitudinal haptic shared control analysis on a fixed base driving simulator*.

Contact Details HREC:
P.O. Box 5015
2600 GA Delft
The Netherlands

HREC@tudelft.nl

Consent Form for:

Longitudinal haptic shared control analysis on a fixed base driving simulator

Please tick the appropriate boxes

Taking part in the study	**YES**	**NO**
I have read and understood the study information dated Monday 3rd May, 2021, or it has been read to me. I have been able to ask questions about the study and my questions have been answered to my satisfaction.	☐	☐
I consent voluntarily to be a participant in this study and understand that I can refuse to answer questions and I can withdraw from the study at any time, without having to provide a reason.	☐	☐
I understand that taking part in the study involves the logging of driving data and the completing of questionnaires.	☐	☐
Risks associated with participating in the study		
I understand that taking part in the study involves the following risks: Emotional discomfort due to the possibility of experiencing a collision scenario.	☐	☐
Use of the information in the study		
I understand that information I provide can be used for presentation in scientific and driving simulator seminars and conferences and published as master theses, PhD theses and articles in scientific journals.	☐	☐
I understand that personal information collected about me that can identify me will not be shared beyond the researchers.	☐	☐
Future use and reuse of the information by others		
I give permission for the driving simulator data that I provide to be archived in TU Delft repository so it can be used for future research and learning	☐	☐

Name of participant	Signature	Date

I have accurately read out the information sheet to the potential participant and, to the best of my ability, ensured that the participant understands to what they are voluntary consenting.

Klaas Koerten

Name of researcher	Signature	Date

Demographics Questionnaire

Demographics Questionnaire:

Longitudinal haptic shared control analysis on a fixed base driving simulator

Please answer the questions truthfully to the best of your ability

What is your age? _____

For how many years do you own a driver's license? _____

How many hours do you drive per week on average? _____

	YES	NO
Do you have prior experience driving with cruise control?	☐	☐

If yes, how many hours of driving per week on average? _____

	YES	NO
Do you have prior experience driving on a driving simulator?	☐	☐

If yes, how many hours? _____

Acceptance Questionnaire

Acceptance Questionnaire:

Haptic shared control to prevent phantom traffic jams

Please tick the appropriate boxes

What is your judgement about the first system you have driven with?

USEFUL	☐ ☐ ☐ ☐ ☐	USELESS
PLEASANT	☐ ☐ ☐ ☐ ☐	UNPLEASANT
BAD	☐ ☐ ☐ ☐ ☐	GOOD
NICE	☐ ☐ ☐ ☐ ☐	ANNOYING
EFFECTIVE	☐ ☐ ☐ ☐ ☐	SUPERFLUOUS
IRRITATING	☐ ☐ ☐ ☐ ☐	LIKEABLE
ASSISTING	☐ ☐ ☐ ☐ ☐	WORTHLESS
UNDESIRABLE	☐ ☐ ☐ ☐ ☐	DESIRABLE
RAISING AWARENESS	☐ ☐ ☐ ☐ ☐	SLEEP-INDUCING

Please tick the appropriate boxes

What is your judgement about the second system you have driven with?

USEFUL	☐ ☐ ☐ ☐ ☐	USELESS
PLEASANT	☐ ☐ ☐ ☐ ☐	UNPLEASANT
BAD	☐ ☐ ☐ ☐ ☐	GOOD
NICE	☐ ☐ ☐ ☐ ☐	ANNOYING
EFFECTIVE	☐ ☐ ☐ ☐ ☐	SUPERFLUOUS
IRRITATING	☐ ☐ ☐ ☐ ☐	LIKEABLE
ASSISTING	☐ ☐ ☐ ☐ ☐	WORTHLESS
UNDESIRABLE	☐ ☐ ☐ ☐ ☐	DESIRABLE
RAISING AWARENESS	☐ ☐ ☐ ☐ ☐	SLEEP-INDUCING

Please tick the appropriate boxes

What is your judgement about the third system you have driven with?

USEFUL	☐ ☐ ☐ ☐ ☐	USELESS
PLEASANT	☐ ☐ ☐ ☐ ☐	UNPLEASANT
BAD	☐ ☐ ☐ ☐ ☐	GOOD
NICE	☐ ☐ ☐ ☐ ☐	ANNOYING
EFFECTIVE	☐ ☐ ☐ ☐ ☐	SUPERFLUOUS
IRRITATING	☐ ☐ ☐ ☐ ☐	LIKEABLE
ASSISTING	☐ ☐ ☐ ☐ ☐	WORTHLESS
UNDESIRABLE	☐ ☐ ☐ ☐ ☐	DESIRABLE
RAISING AWARENESS	☐ ☐ ☐ ☐ ☐	SLEEP-INDUCING